Neuron

Article

Ventral hippocampal parvalbumin interneurons gate the acute anxiolytic action of the serotonergic psychedelic DOI

Graphical abstract

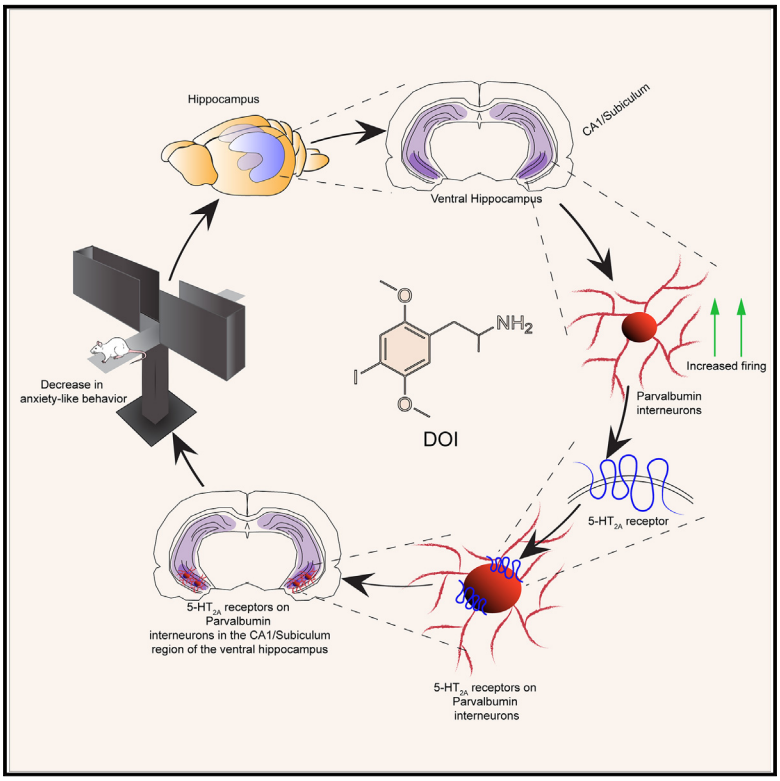

Highlights

- The psychedelic DOI evokes acute anxiolytic effects in rodent models via the vHpc
- DOI enhances the firing rate of a fast-spiking neuron subpopulation in the vHpc
- Opto-tagging reveals that DOI recruits PV-positive inhibitory interneurons in the vHpc
- Agonism of 5-HT$_{2A}$ receptors on PV neurons in the vHpc mediates DOI-evoked anxiolysis

Authors

Praachi Tiwari, Pasha A. Davoudian, Darshana Kapri, ..., Antonio Fernandez-Ruiz, Alex C. Kwan, Vidita A. Vaidya

Correspondence

praachi.tiwari@tifr.res.in (P.T.), vvaidya@tifr.res.in (V.A.V.)

In brief

Tiwari et al. identify the discrete neural circuit underlying the acute anxiolytic actions of the serotonergic psychedelic DOI, demonstrating that DOI recruits 5-HT$_{2A}$ receptors on parvalbumin-positive, fast-spiking inhibitory interneurons in the ventral hippocampal CA1/subiculum region to drive its acute anxiolytic effects.

Tiwari et al., 2024, Neuron *112*, 1–18
November 20, 2024
https://doi.org/10.1016/j.neuron.2024.08.016

CellPress

Neuron

CellPress

Article

Ventral hippocampal parvalbumin interneurons gate the acute anxiolytic action of the serotonergic psychedelic DOI

Praachi Tiwari,[1,10,*] Pasha A. Davoudian,[2,3] Darshana Kapri,[1] Ratna Mahathi Vuruputuri,[1] Lindsay A. Karaba,[4] Mukund Sharma,[1] Giulia Zanni,[5,6] Angarika Balakrishnan,[1] Pratik R. Chaudhari,[1] Amartya Pradhan,[1] Shital Suryavanshi,[1] Kevin G. Bath,[5,6] Mark S. Ansorge,[5,6] Antonio Fernandez-Ruiz,[4] Alex C. Kwan,[7,8,9] and Vidita A. Vaidya[1,11,*]

[1]Department of Biological Sciences, Tata Institute of Fundamental Research, Mumbai 400005, India
[2]Medical Scientist Training Program, Yale University School of Medicine, New Haven, CT 06511, USA
[3]Interdepartmental Neuroscience Program, Yale University School of Medicine, New Haven, CT 06511, USA
[4]Department of Neurobiology and Behavior, Cornell University, Ithaca, NY, USA
[5]Department of Psychiatry, Columbia University, New York, NY 10032, USA
[6]Department of Developmental Neuroscience, New York State Psychiatric Institute, New York, NY 10032, USA
[7]Department of Psychiatry, Yale University School of Medicine, New Haven, CT 06511, USA
[8]Meinig School of Biomedical Engineering, Cornell University, Ithaca, NY 14853, USA
[9]Department of Psychiatry, Weill Cornell Medicine, New York, NY 10065, USA
[10]Present address: Department of Psychiatry and Behavioral Sciences, Johns Hopkins University, Baltimore, MD, USA
[11]Lead contact
*Correspondence: praachi.tiwari@tifr.res.in (P.T.), vvaidya@tifr.res.in (V.A.V.)
https://doi.org/10.1016/j.neuron.2024.08.016

SUMMARY

There has been a recent renewal of interest in the therapeutic potential of serotonergic psychedelics. Here, we uncover the essential role of ventral hippocampus (vHpc) GABAergic interneurons in the anxiolytic effect evoked by the serotonergic psychedelic 2,5-dimethoxy-4-iodoamphetamine (DOI). Integrating anatomical, pharmacological, and genetic approaches, we show that 5-HT_{2A} receptors in the CA1/subiculum (CA1/sub) region of the vHpc are required for the anxiolytic action of DOI. *In vivo* electrophysiology and opto-tagging experiments indicate that DOI enhances the firing rate of hippocampal fast-spiking parvalbumin (PV)-positive interneurons, most of which express the 5-HT_{2A} receptors. Restoration of 5-HT_{2A} receptors in PV-positive interneurons in a loss-of-function background reinstated the anxiolytic responses evoked by DOI in the vHpc CA1/sub region. Collectively, our results localize the acute anxiolytic action of a serotonergic psychedelic to 5-HT_{2A} receptors in the ventral hippocampus and specifically identify PV-positive fast-spiking cells as a cellular trigger for the psychedelic-induced relief of anxiety-like behavior.

INTRODUCTION

There has been a resurgence of interest in serotonergic psychedelics as potential therapeutic agents for mental illnesses.[1–4] Studies with humans indicate that serotonergic psychedelics exert hallucinatory effects via their agonist action at the serotonin$_{2A}$ (5-HT_{2A}) receptor.[5] In addition to their ability to alter sensory perception acutely, clinical studies also suggest that serotonergic psychedelics can evoke persistent therapeutic effects in patients with generalized anxiety disorder, as well as post-traumatic stress disorder and treatment-resistant major depression.[2,6–9] Evidence from rodent models indicates that several serotonergic psychedelics can reduce anxiety-like behavior in ethologically relevant assays such as the elevated plus maze (EPM).[10–13] However, the neural substrate and importance of 5-HT_{2A} receptors in mediating this aspect of the behavioral effects of serotonergic psychedelics have not been elucidated.

Prior preclinical studies with 2,5-dimethoxy-4-iodoamphetamine (DOI), a partial agonist of the 5-HT_{2A} receptor and a classic phenethylamine psychedelic,[14,15] indicate that acute systemic administration of DOI robustly reduces anxiety-like behavior.[12,13] By contrast, systemic administration of lysergic acid diethylamide (LSD) does not alter anxiety-like behavior in stress-naive mice, but with chronic dosing can ameliorate stress-induced anxiety-like behavior.[10] Given the differential affinities for distinct 5-HT receptors, diverse serotonergic psychedelics are thought to exert both unique, as well as overlapping, behavioral effects.[16,17] Thus far, these studies converge to suggest related anxiolytic actions for different serotonergic psychedelics but do not provide a detailed understanding of the underlying neural mechanism.

Please cite this article in press as: Tiwari et al., Ventral hippocampal parvalbumin interneurons gate the acute anxiolytic action of the serotonergic psychedelic DOI, Neuron (2024), https://doi.org/10.1016/j.neuron.2024.08.016

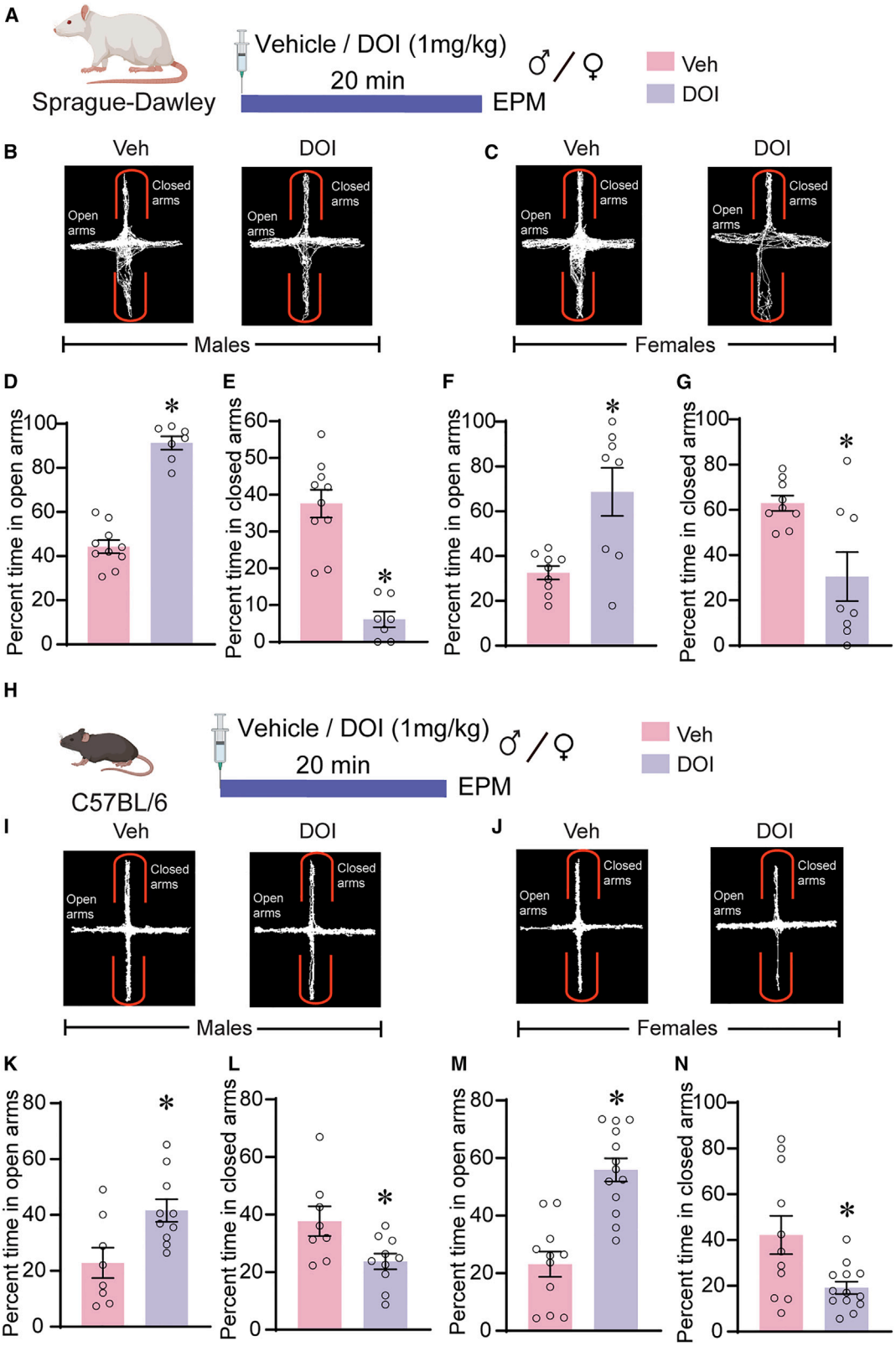

(legend on next page)

In this study, we seek to identify the specific brain region, neuronal cell type, and receptor that triggers the relief of anxiety-like behavior following DOI treatment. Through a series of systematic investigations involving rats and mice, systemic and localized drug administrations, pharmacological blockade, electrophysiology, and opto-tagging, as well as knockout mouse models, we provide evidence to pinpoint a critical role for 5-HT_{2A} receptors on parvalbumin (PV)-positive interneurons of the ventral hippocampus (vHpc) in mediating the DOI-evoked anxiolytic response.

RESULTS

Acute systemic administration of DOI decreases anxiety-like responses on the EPM

We first examined whether a single administration of DOI can alter anxiety-like behavior on the EPM in both male and female rats, as well as mice (Figures 1A and 1H). Both male and female rats acutely administered DOI (1 mg/kg) exhibited robust anxiolytic responses on the EPM, as indicated by a significant increase in percent time spent in the open arms (male rats: $p < 0.0001$; female rats: $p = 0.012$) and a significant decrease in percent time spent in the closed arms (male rats: $p < 0.0001$; female rats: $p = 0.02$) (Figures 1A–1G). The robust decline in anxiety-like behavior was noted across all bins (5 min) in a 15-min behavioral paradigm (Figures S1A–S1C). We also noted a significant reduction in locomotion in the EPM in DOI-treated rats (male rats: $p < 0.0001$; female rats: $p < 0.0001$) (Figures S1D and S1E). The effects of DOI on anxiety-like behavior on the EPM did not persist 24 h post administration (Figures S1H–S1J). The acute anxiolytic actions of DOI were also noted on a modified EPM task, with a heightened difference in light intensity between open and closed arms task ($p < 0.0001$; Mann-Whitney U test) (Figures S1F and S1G).

Similar to the effects noted in rats, male and female C57BL/6 mice also exhibited a robust reduction in anxiety-like behavior on the EPM following acute DOI (1 mg/kg) treatment (Figures 1H–1N), with a significant increase in percent time in the open arms (male mice: $p = 0.012$; female mice: $p < 0.0001$) and a significant decrease in percent time in the closed arms (male mice: $p = 0.021$; female mice: $p = 0.022$) (Figures 1I–1N). The acute anxiolytic effect of DOI on mice was also noted on the modified EPM ($p < 0.0001$; Mann-Whitney test) (Figure S1N). In contrast to the DOI-evoked reduction in locomotion in rats, C57BL/6 mice exhibited increases in locomotion on the EPM (male mice: $p = 0.022$; female mice: $p = 0.005$) (Figures S1K–S1M).

These results indicate that acute systemic administration of DOI evokes robust decreases in anxiety-like behaviors on the EPM in male and female rats, as well as mice, while inducing species-specific effects on total locomotion.

Direct infusion of DOI into the CA1/sub field of the vHpc evokes anxiolysis

The interconnected network of the medial prefrontal cortex (mPFC), hippocampus, and amygdala plays a key role in the control of anxiety-like behavior. We sought to address whether direct infusion of DOI into these brain regions can phenocopy the systemic DOI-evoked anxiolysis. Direct infusion of DOI (1 μg/μL per hemisphere) using cannula implants into the prelimbic (PrL) or infralimbic (IL) mPFC subdivisions, basal amygdala (BA), or dorsal hippocampus (dHpc) CA1/subiculum (sub) region did not alter anxiety-like behavior or total locomotion on the EPM (Figures S2A–S2S). By contrast, direct DOI infusion in the vHpc CA1/sub region, in both male and female rats, evoked significant decreases in anxiety-like behavior, with an increase in percent time in the open arms (male rats: $p = 0.004$; female rats: $p = 0.005$) and decreased percent time in the closed arms (male rats: $p = 0.005$; female rats: $p = 0.003$) (Figures 2A–2H), but did not influence the total distance traveled in either male or female rats (Figures S3A–S3C). Direct infusion of DOI into the vHpc CA1/sub region of rats also evoked a decline in anxiety-like behavior on another approach-avoidance behavioral task, the open field (OF) test, with significant increases in percent time ($p < 0.0001$) and frequency of visits to the center ($p = 0.008$) of the OF arena, with no change in total locomotion (Figures S3E–S3G). Similar anxiolytic effects were noted in C57BL/6 mice following DOI infusion in the vHpc CA1/sub region, with a significant increase in percent time in the open arms ($p = 0.034$) and a decrease in percent time in the closed arms ($p = 0.022$) of the EPM, as well as a significant increase in percent time ($p = 0.042$) and frequency of visits to the center ($p = 0.046$) of the OF arena (Figures S3H–S3N). Further, we find that local delivery of DOI in the vHpc CA1/sub region does not evoke the classical head twitch response (HTR) evoked by serotonergic psychedelics (Figure S3D), suggesting that this behavioral signature likely involves neural circuits other than vHpc CA1/sub region.

Taken together, these results indicate that direct infusion of DOI into the vHpc CA1/sub region evokes robust and significant

Figure 1. Acute systemic administration of DOI decreases anxiety-like responses on the elevated plus maze

(A) Shown is a schematic for the experimental paradigm to explore the acute effects of DOI (1 mg/kg) administration in male and female rats on the EPM.

(B) Shown are the tracks on the EPM for a representative vehicle (left) or DOI (right) treated male rat (Veh:$n = 10$; DOI:$n = 7$).

(C) Shown are the tracks on the EPM for a representative vehicle (left) or DOI (right) treated female rat (Veh:$n = 9$; DOI:$n = 8$).

(D–G) Male and female rats treated with DOI show significant increases in the time spent in the open arms (D:$F_{(9,6)} = 1.43$; F:$F_{(7,8)} = 11.48$), and significant decreases in time spent in the closed arms (E:$F_{(9,6)} = 4.47$; G:$F_{(7,8)} = 9.04$) of the EPM.

(H) Shown is a schematic for the experimental paradigm to explore the acute effects of DOI (1 mg/kg) administration in male and female mice (C57BL/6) on the EPM.

(I) Shown are the tracks on the EPM for a representative vehicle (left) or DOI (right) treated male mouse (Veh:$n = 8$; DOI:$n = 10$).

(J) Shown are the tracks on the EPM for a representative vehicle (left) or DOI (right) treated female mouse (Veh:$n = 11$; DOI:$n = 13$).

(K–N) Male and female mice treated with DOI show significant increases in the time spent in the open arms (K:$F_{(7,9)} = 1.44$; M:$F_{(10,12)} = 1.19$), and significant decreases in the time spent in the closed arms (L:$F_{(7,9)} = 2.80$; N:$F_{(10,12)} = 6.59$) of the EPM.

*$p < 0.05$. Hollow circles represent individual data points. Data are mean ± SEM.

See also Figure S1.

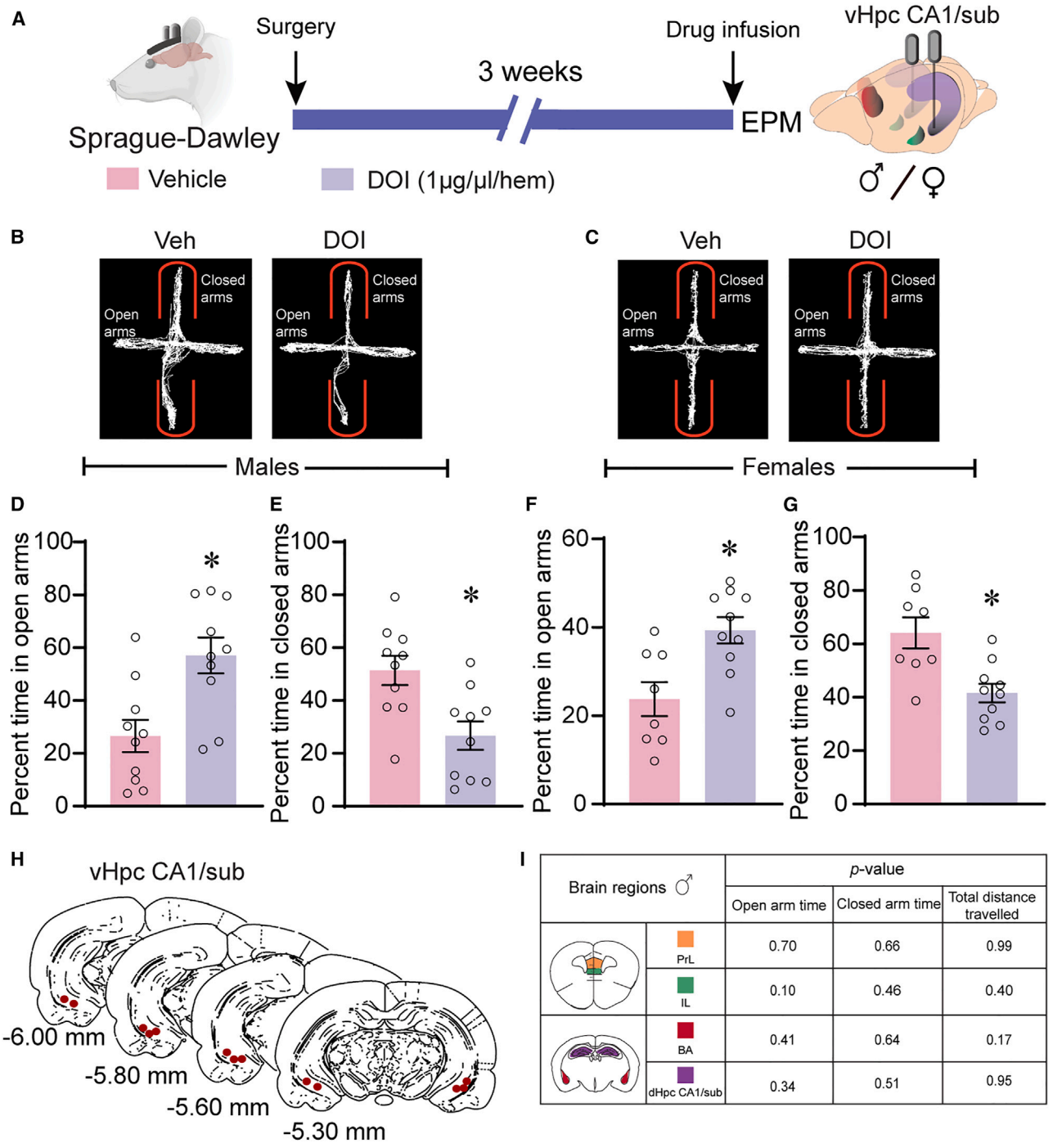

I

Brain regions ♂		*p*-value		
		Open arm time	Closed arm time	Total distance travelled
	PrL	0.70	0.66	0.99
	IL	0.10	0.46	0.40
	BA	0.41	0.64	0.17
	dHpc CA1/sub	0.34	0.51	0.95

Figure 2. Direct infusion of DOI into the CA1/subiculum field of the ventral hippocampus evokes anxiolysis

(A) Shown is a schematic for the experimental paradigm to deliver vehicle or DOI (1 μg/μL per hemisphere) in the vHpc CA1/sub region in Sprague-Dawley rats using cannula infusion systems prior to subjecting animals to behavioral analysis on the EPM.

(B) Shown are the tracks on the EPM for a representative vehicle (left) or DOI (right) treated male rat (right) (Veh:*n* = 10, DOI:*n* = 10).

(C) Shown are the tracks on the EPM for a representative vehicle (left) or DOI (right) treated female rat (Veh:*n* = 8, DOI:*n* = 10).

(D–G) Male and female rats subjected to bilateral delivery of DOI in the vHpc CA1/sub region show a significant increase in the time spent in the open arms ($D:F_{(9,9)} = 1.23$; $F:F_{(7,9)} = 1.34$), and a significant decrease in the time spent in the closed arms ($E:F_{(9,9)} = 1.06$; $G:F_{(7,9)} = 2.25$) of the EPM.

(H) Shown is a schematic representation of cannula placement in the vHpc CA1/sub region in male rats. Red dots represent the position of the tip of the implanted cannulas.

(legend continued on next page)

Please cite this article in press as: Tiwari et al., Ventral hippocampal parvalbumin interneurons gate the acute anxiolytic action of the serotonergic psychedelic DOI, Neuron (2024), https://doi.org/10.1016/j.neuron.2024.08.016

decreases in anxiety-like behavior on the EPM, implicating the vHpc CA1/sub region in DOI-evoked anxiolysis. By contrast, direct infusion of DOI into the PrL or IL subdivisions of the mPFC, BA, or the CA1/sub region of the dHpc does not influence anxiety-like behavior (Figure 2I).

5-HT_{2A} receptors in the vHpc CA1/sub region mediate the decrease in anxiety-like behavior evoked by DOI

Given that DOI is a partial agonist of the 5-HT_2 receptor family, with a greater affinity for the 5-HT_{2A} receptor, we employed a pharmacological approach to examine the contribution of 5-HT_{2A} receptors in the vHpc CA1/sub region in mediating the anxiolytic effects of systemic DOI treatment. MDL100907 (MDL), a selective 5-HT_{2A} receptor antagonist, was directly delivered into the vHpc CA1/sub region prior to systemic DOI administration in rats, followed by behavioral analysis on the EPM (Figures 3A and 3B). Two-way ANOVA analysis revealed a significant DOI × MDL interaction effect for percent time in the open arms (p = 0.016) (Figure 3C). Post hoc analyses indicated that MDL + DOI cohort did not exhibit the decrease in anxiety-like behavior noted in the DOI-treated animals. Two-way ANOVA analysis also indicated a significant DOI × MDL interaction effect (p = 0.017) and a significant main effect of MDL ($F_{(1,27)}$ = 6.59, p = 0.016) for percent time in the closed arms of the EPM (Figure 3D). Post hoc analyses indicated that the DOI-treated group spent significantly lower percent time in the closed arms compared with the MDL + DOI cohort (Figure 3D). We observed no significant DOI × MDL interaction effect for total locomotion in the EPM. However, we noted a significant main effect of systemic DOI treatment for total locomotion in the maze ($F_{(1,27)}$ = 8.98, p = 0.006) (Figures S4A and S4B), with a decrease in total distance moved in both DOI and MDL + DOI cohorts. These results indicate that while the decrease in anxiety-like behavior on the EPM with systemic DOI administration involves a critical role for 5-HT_{2A} receptors in the vHpc CA1/sub region, it is likely that the reduced total locomotion is mediated via other neurocircuits.

We next sought to confirm the contribution of 5-HT_{2A} receptors in the vHpc CA1/sub region to DOI-evoked anxiolytic behavior in the EPM using a genetic strategy. We capitalized on wild-type (WT) and 5-HT_{2A}RKO mouse lines, which were subjected to direct infusion of vehicle or DOI into the vHpc CA1/sub region (Figures 3E and 3F). Two-way ANOVA analysis revealed a significant 5-HT_{2A}RKO × DOI interaction for percent time in the open arms (p = 0.037), as well as percent time in the closed arms (p = 0.032) (Figures 3G–3I). We also noted a significant main effect of DOI for percent time in the closed arms ($F_{(1,27)}$ = 10.14, p = 0.004). Post hoc analyses indicated that while DOI evoked a significant decrease in the percent time spent in the closed arms in the WT cohort, this effect of DOI on anxiety-like behavior was lost in the 5-HT_{2A}RKO mice.

We then asked whether a restoration of 5-HT_{2A} receptor expression within the vHpc CA1/sub region in the 5-HT_{2A}RKO mouse line was sufficient to result in anxiolytic behavioral responses on the EPM in response to acute, systemic DOI treatment. Using a viral delivery approach with AAV9-Syn-Cre-GFP infusion into the vHpc CA1/sub region of 5-HT_{2A}RKO-res$^{fl/fl}$ mouse line, we restored neuronal 5-HT_{2A} receptor expression in the vHpc CA1/sub region in a 5-HT_{2A}R receptor loss-of-function background.[18] The Cre-recombinase acts through an excision of the floxed neostop cassette that lies upstream of the *htr2a* gene, which facilitates a conditional restoration of 5-HT_{2A} receptor expression in neurons that express synapsin-Cre (Figures S4C and S4D). We noted that acute, systemic DOI administration in 5-HT_{2A}RKO-res$^{fl/fl}$ mice with a Cre-recombinase mediated rescue of 5-HT_{2A} receptor expression in neurons within the vHpc CA1/sub region resulted in a significant decline in anxiety-like behavior on the EPM, as observed with an increase in percent time in the open arms (p = 0.014) and a reduction in percent time in the closed arms (p = 0.004) (Figures S4E–S4G).

These results, based on both pharmacological strategies in rat models and a genetic loss-of-function approach in mice, collectively indicate that DOI exerts a robust influence on anxiety-like behavior through 5-HT_{2A} receptors in the vHpc CA1/sub region.

Acute systemic administration of DOI alters single-unit firing rates in the vHpc CA1/sub region *in vivo*

Given that the 5-HT_{2A} receptors in the vHpc are expressed in multiple cell types, we next sought to explore the influence of systemic DOI administration on millisecond-level spiking activity using large-scale electrophysiology. High-density neuropixels silicon probes[19] were inserted targeting the vHpc CA1/sub region in C57BL/6 mice to record spiking activity before and after the administration of DOI or vehicle (Figures 4A, 4B, S5A, and S5B). We isolated single units and classified them based on peak-to-trough duration (Figure 4C) to separate putative regular spiking (RS) and fast-spiking (FS) neurons.[20,21] As expected, we found that FS neurons have a higher firing rate at baseline compared with RS neurons (Figure 4D, $p = 2.88 \times 10^{-6}$). Consistent with prior reports[22] ~20% of the recorded single units were classified as FS neurons (Figure 4D). To determine the effect of DOI on neural firing dynamics, we normalized the post-injection changes in firing rates into Z scores for RS and FS cell classes following either DOI or vehicle administration (Figure 4E). The analyses revealed that many RS and FS neurons increased their spike rates rapidly following systemic DOI administration. To determine if the firing changes were statistically significant, we determined the fractions of neurons with a Z score change of ≤ 5 or ≥ 5. DOI administration led to a significantly higher number of cells with increased firing rates, including both RS and FS subtypes (Figure 4F). Proportionally, there were more FS neurons excited than RS neurons after DOI administration. These results indicate that DOI administration can rapidly increase the spiking activity in the vHpc, including in a select subpopulation of FS neurons.

(I) Table summarizing the p values analyzed using unpaired Student's t test for anxiety-related measures on the EPM when DOI was directly infused in the PrL and IL regions of the mPFC, the dHpc CA1/sub region, and the BA.

*$p < 0.05$. Hollow circles represent individual data points. Data are mean ± SEM.

See also Figures S2 and S3.

Please cite this article in press as: Tiwari et al., Ventral hippocampal parvalbumin interneurons gate the acute anxiolytic action of the serotonergic psychedelic DOI, Neuron (2024), https://doi.org/10.1016/j.neuron.2024.08.016

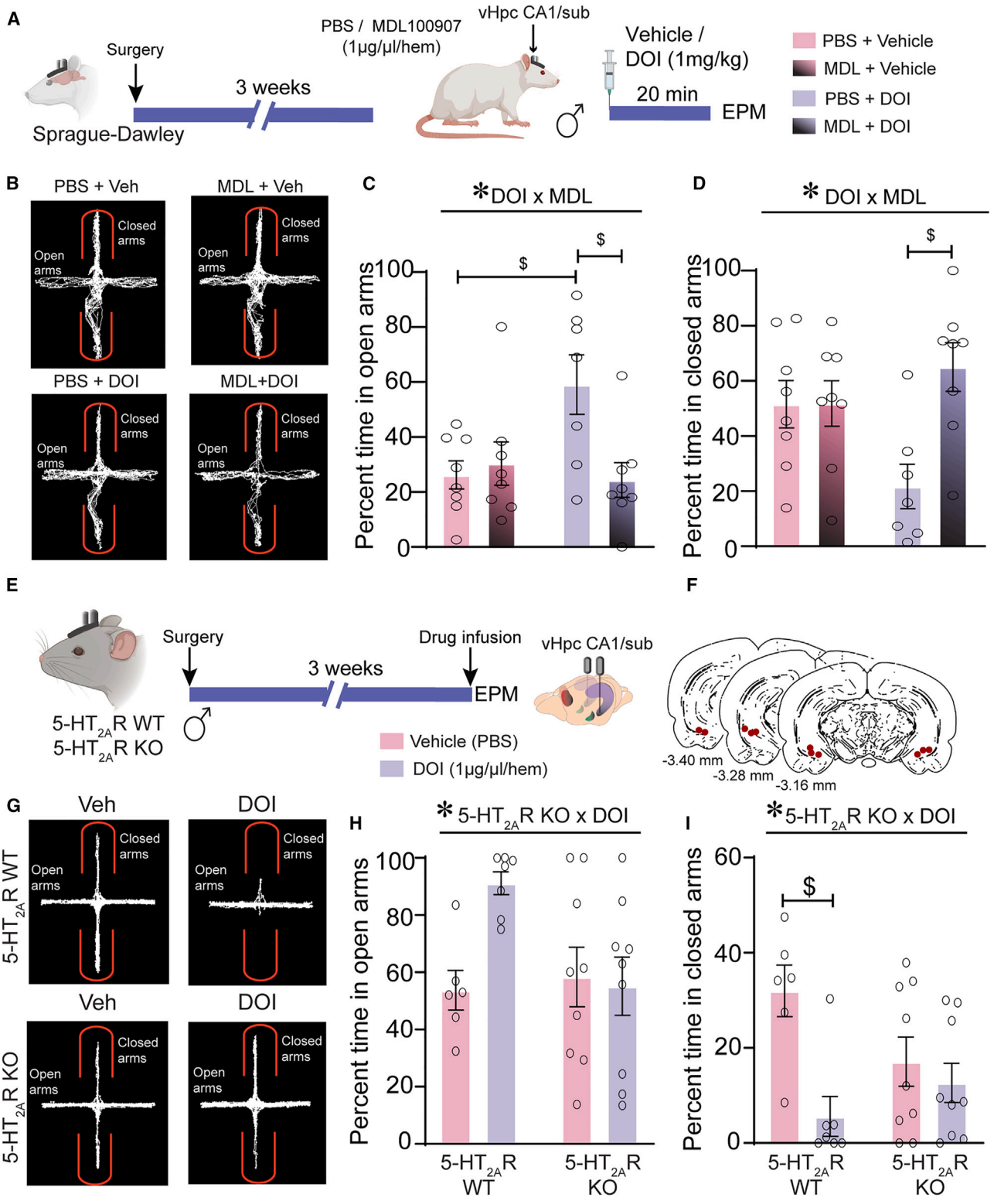

Figure 3. 5-HT$_{2A}$ receptors in the ventral hippocampal CA1/sub region mediate the decrease in anxiety-like behavior evoked by DOI

(A) Shown is a schematic for the experimental paradigm for direct infusion of PBS or MDL100907 (1 μg/μL per hemisphere) in the vHpc CA1/sub region prior to subjecting animals to a systemic vehicle or DOI (1 mg/kg) treatment followed by behavioral analysis on the EPM.

(legend continued on next page)

Please cite this article in press as: Tiwari et al., Ventral hippocampal parvalbumin interneurons gate the acute anxiolytic action of the serotonergic psychedelic DOI, Neuron (2024), https://doi.org/10.1016/j.neuron.2024.08.016

5-HT$_{2A}$ receptors are expressed on both excitatory and inhibitory neurons of the vHpc

Our findings reveal that 5-HT$_{2A}$ receptors in the vHpc CA1/sub region play a role in the DOI-induced reduction of anxiety-like behavior on the EPM, which is accompanied by DOI-evoked increases in firing rate of FS neurons in the vHpc CA1/sub region. Nonetheless, the specific neuronal cell types within the vHpc that express 5-HT$_{2A}$ receptors remain unclear. Thus, we aimed to use RNAscope to examine the *Htr2a* expression in PV-positive and CamKIIα-positive neurons in the vHpc CA1/sub region of C57BL/6 mice. We find that *Htr2a* is ubiquitously expressed in both neuronal cell types (Figure 5A). Previous work indicates that at a single-cell resolution, mRNA expression is visualized both as puncta and clusters.[23] Therefore, we assessed both puncta and clusters of *Htr2a* expression on PV-positive and CamKIIα-positive neurons. We find that the levels of expression of both *Htr2a* puncta ($p = 0.0349$) and clusters ($p = 0.0263$) were significantly higher in PV-positive neurons as compared with CamKIIα-positive neurons ($p < 0.0001$) (Figure 5B), with as many as 98% of PV-positive neurons expressing *Htr2a* mRNA and about 67% of CamKIIα-positive neurons exhibiting *Htr2a* expression ($p = 0.0005$) (Figure 5C).

We next sought to employ an immunofluorescence approach with the neuronal activation marker, c-Fos, to assess the induction of c-Fos expression by DOI in PV and CamKIIα-positive neurons within the vHpc CA1/sub region of C57BL/6 mice (Figures 5D–5H). Double immunofluorescence studies reveal that following acute DOI treatment, there was a significant increase in the expression of c-Fos in PV-positive neurons ($p < 0.0001$) (Figures 5E, 5F, and S6A–S6D), which was not observed in the CamKIIα-positive neurons (Figures 5G and 5H).

5-HT$_{2A}$ receptors on PV-positive inhibitory interneurons in the vHpc CA1/sub region contribute to the DOI-evoked decline in anxiety-like behavior on the EPM

Given evidence from our neuropixel recordings that acute DOI administration enhances firing of FS neurons in the vHpc CA1/sub region, which are likely to be PV-positive inhibitory interneurons[24] that express 5-HT$_{2A}$ receptors, we next sought to directly address whether acute DOI influences activity of PV-positive neurons in this region. To address this, we capitalized on an opto-tagging approach to identify PV-positive neurons using chronic probes with optical fibers implanted in the vHpc CA1/sub region of bigenic mice that expressed channelrhodopsin 2 (ChR2) in PV-positive interneurons (PV::ChR2) (Figures 6A–6C). Using spike width and burstiness, we sorted cells into different subclasses of neurons and identified the opto-tagged PV-positive neurons, putative PV-negative neurons, and pyramidal neurons. We confirmed the activation of PV-positive neurons with opto-stimulation (Figures 6D and 6E). On acute DOI administration, we noted a significant increase in firing of a higher fraction of opto-tagged PV-positive neurons ($p < 0.001$), indicating that the neurons that are engaged in the vHpc CA1/sub region by DOI are PV-positive interneurons (Figure 6F).

While our results reveal that acute DOI administration enhances firing of PV-positive neurons in the vHpc CA1/sub, it is unclear whether PV-positive neurons within this region influence anxiety-like behavior on the EPM.[23] To address the possibility that activation of PV-positive neurons within the vHpc CA1/sub region may phenocopy the anxiolytic actions of DOI on the EPM, we capitalized on a chemogenetic strategy. We performed stereotactic surgery in the vHpc CA1/sub region of a PV-Cre mouse line to bilaterally deliver an adenoviral construct that contained a double-floxed inverted open reading frame (DIO) incorporating the hM3Dq-DREADD (designer receptors exclusively activated by designer drugs) or the hM4Di-DREADD under the control of a human synapsin promoter (rAAV2-hSyn-DIO-hM3Dq-mCherry or rAAV2-hSyn-DIO-hM4Di-mCherry). Mice expressing the hM3Dq-DREADD virus in PV-positive interneurons in the vHpc CA1/sub region were systemically administered the DREADD actuator clozapine-N-oxide (CNO) or vehicle prior to behavioral analysis on the EPM (Figures 7A–7D, S7A, and S7B). We observed a decrease in anxiety-like behavior in CNO-treated mice, as noted with a significant increase in percent time in the open arms ($p = 0.0005$), as well as decrease in percent time in the closed arms ($p = 0.002$) (Figures 7C and 7D). By contrast, mice expressing the hM4Di-DREADD virus in PV-positive interneurons in the vHpc CA1/sub region show enhanced anxiety-like behavior on the EPM in response to systemic CNO administration (Figures 7E–7H, S7D, and S7E), with a significant decrease noted in percent time in the open arms ($p = 0.005$) and as well as an increase in percent time in the closed arms ($p = 0.021$) (Figures 7G and 7H). We noted no difference in total locomotion between treatment groups in both

(B) Shown are the tracks on the EPM for individual representative rats from different treatment groups, namely: PBS + vehicle (upper, left), MDL + vehicle (upper, right), PBS + DOI (lower, left), and MDL + DOI (lower, right) (PBS + Veh:$n = 8$, MDL + Veh:$n = 8$, PBS + DOI:$n = 7$, DOI + MDL:$n = 8$).

(C and D) Male rats pretreated with a direct infusion of MDL into the vHpc CA1/sub region showed a significant blockade of the decrease in anxiety-like behavior evoked by systemic DOI treatment on EPM. The systemic DOI-evoked increase in percent time in the open arms (C: $F_{(1,27)} = 6.48$) and the DOI-evoked decrease in percent time in the closed arms (D: $F_{(1,27)} = 6.42$) were not observed in the MDL + DOI treatment cohort. F-values are indicated for DOI × MDL interaction effect.

(E) Shown is a schematic for the experimental paradigm to deliver DOI (1 μg/μL per hemisphere) in the vHpc CA1/sub region in 5-HT$_{2A}$R KO and wild-type (WT) mice prior to subjecting the animals to behavioral analysis on the EPM.

(F) Shown is a schematic representation of cannula placement in vHpc CA1/sub region in mice. Red dots represent the position of the tip of the implanted cannulas.

(G) Shown are the tracks on the EPM for a representative 5-HT$_{2A}$R WT and 5-HT$_{2A}$R KO mouse treated with either vehicle (left, upper, and lower) or DOI (right, upper, and lower) (5-HT$_{2A}$R WT-Veh:$n = 6$, DOI:$n = 7$; 5-HT$_{2A}$R KO-Veh:$n = 9$, DOI:$n = 9$).

(H and I) 5-HT$_{2A}$R KO male mice with a direct infusion of DOI into the vHpc CA1/sub region did not exhibit any change in anxiety-like behavior on the EPM, with no change in percent time in the open (H:$F_{(1,27)} = 4.83$) or closed arms (I:$F_{(1,27)} = 5.13$), unlike the DOI-evoked anxiolysis noted in 5-HT$_{2A}$R WT male mice. F-values are listed for 5-HT$_{2A}$R KO × DOI interaction effect.

*$p < 0.05$; *DOI × MDL and *5-HT$_{2A}$RKO × DOI indicate a significant two-way ANOVA interaction. $^{\$}p < 0.05$ Bonferroni's post hoc test. Hollow circles represent individual data points. Data are mean ± SEM.

See also Figure S4.

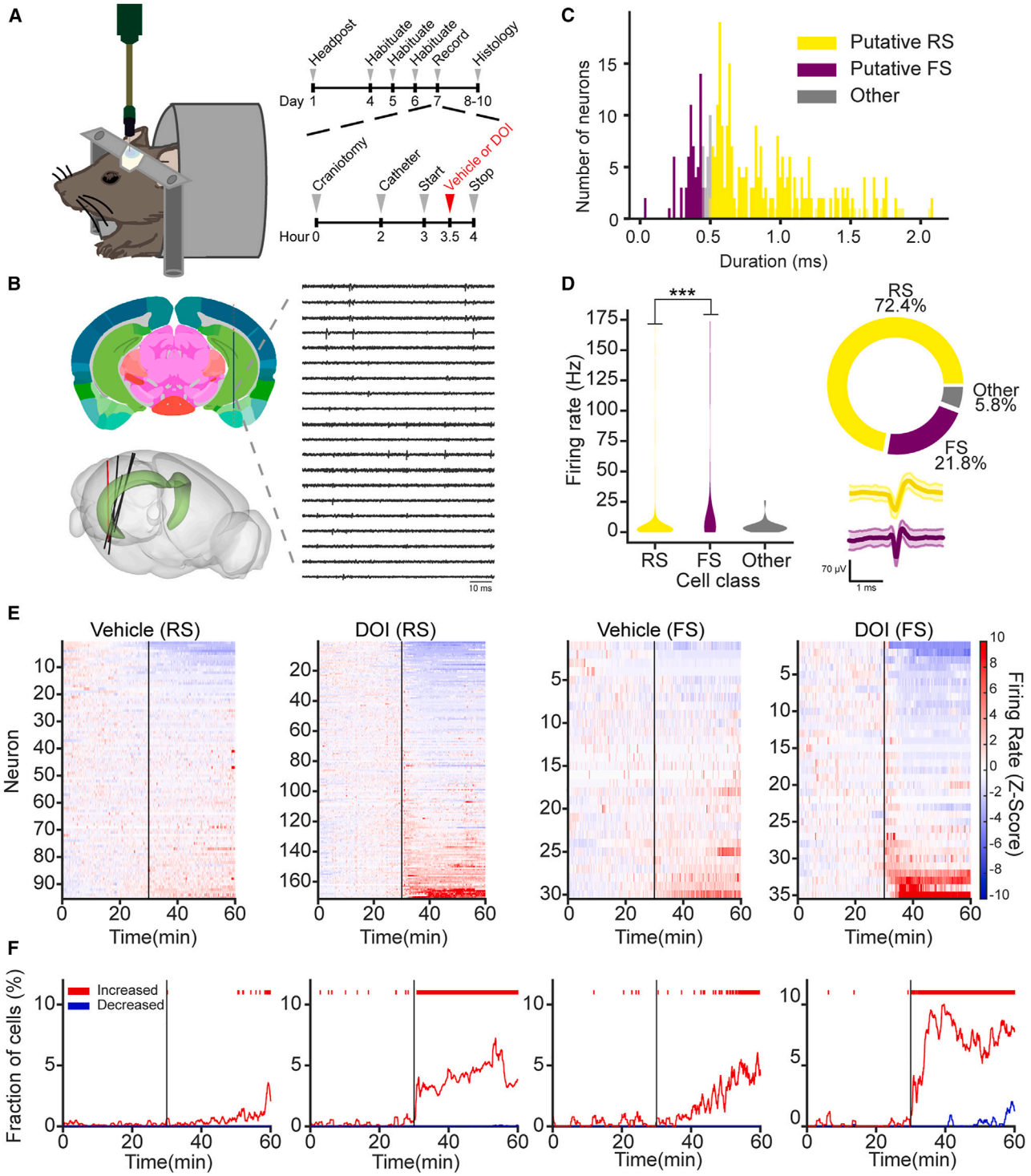

Figure 4. Acute systemic administration of DOI alters single-unit firing rates in the ventral hippocampal CA1/sub region *in vivo*

(A) Schematic of *in vivo* physiology recordings. Left: awake, head-fixed mouse with neuropixel probe in vHpc. Right: timeline of surgery and experiment.

(B) Targeting vHpc for *in vivo* electrophysiology. Left: targeted path for insertion of neuropixels probe. Bottom: reconstructed three-dimensional path of probe.

(C) Separation of regular (RS) and fast-spiking (FS) neurons. Top: distribution of spike width duration and classification of putative RS and FS neurons.

(D) Separation of RS and FS neurons. Left: violin plots demonstrate that FS cells have increased firing rate frequency compared with RS neurons. Right: distribution of RS and FS neurons in dataset (top) and representative single-unit examples of each (bottom).

(E) Firing rate *Z* score changes from RS and FS neurons after systemic treatment with either vehicle or DOI.

(legend continued on next page)

experiments (Figures S7C and S7F). We next sought to assess potential off-target effects of CNO (5 mg/kg), for which PV-Cre mice were bilaterally administered an adenovirus with a non-DREADD sequence (rAAV2-hsyn-DIO-mCherry) in the vHpc CA1/sub region prior to CNO treatment and behavioral analysis. CNO administration evoked no change in any behavioral measure on the EPM as compared with vehicle-treated mice (Figures S7G–S7K). Taken together, these results indicate that DOI administration activates PV-positive inhibitory interneurons in the vHpc CA1/sub region and that chemogenetic activation of these neurons can evoke a decline in anxiety-like behavior on the EPM, whereas chemogenetic inhibition results in an increase in anxiety-like behavior on the EPM.

We then addressed whether the DOI-evoked reduction in anxiety-like behavior on the EPM involves a key role for 5-HT_{2A} receptor expressing PV-positive inhibitory interneurons in the vHpc CA1/sub region (Figure 8A). In order to address this, we generated a PV-Cre::5-HT_{2A}RKO-res$^{fl/fl}$ bigenic mouse line (Figure 8A, upper), with a selective restoration of 5-HT_{2A} receptors in PV-positive neurons, in a 5-HT_{2A} receptor loss-of-function background (Figures 8B, S8A, and S8B). We directly infused DOI into the vHpc CA1/sub region of PV-Cre::5-HT_{2A}RKO-res$^{fl/fl}$ bigenic mice prior to analyzing behavior on the EPM (Figure 8A, lower). We observed a significant reduction in anxiety-like behavior in DOI-treated PV-Cre::5-HT_{2A}RKO-res$^{fl/fl}$ bigenic mice, with a significant increase in percent time in the open arms ($p = 0.029$) and a decrease in percent time in the closed arms ($p = 0.043$) (Figures 8C–8E). We did not observe any change in total locomotion on the EPM in PV-Cre::5-HT_{2A}RKO-res$^{fl/fl}$ bigenic mice following direct DOI infusion (Figure S8C). These results indicate that the selective restoration of 5-HT_{2A} receptors in PV-positive neurons, in a 5-HT_{2A} receptor loss-of-function background, can reinstate the anxiolytic behavioral responses noted following direct infusion of DOI into the vHpc CA1/sub region, which are lost in 5-HT_{2A}RKO mice (Figures 3E–3I).

We further sought to examine whether a restoration of 5-HT_{2A} receptor expression within CamKIIα-positive neurons of the vHpc CA1/sub region in the 5-HT_{2A}RKO mouse line can influence anxiolytic behavioral responses on the EPM in response to acute, systemic DOI treatment (Figures S8D–S8I). Using a Cre-based viral approach (AAV9-CamKII-GFP-Cre), targeting the vHpc CA1/sub region of 5-HT_{2A}RKO-res$^{fl/fl}$ mouse line, we restored neuronal 5-HT_{2A} receptor expression in CamKIIα neurons of the vHpc CA1/sub region in a 5-HT_{2A}R receptor loss-of-function background (Figures S8D and S8E). We noted that acute, systemic DOI administration in these animals did not influence anxiety-like behavior on the EPM (Figures S8F–S8I).

Collectively, our results indicate that PV-positive inhibitory interneurons in the vHpc CA1/sub region influence anxiety-like behavior, with activation of PV-positive interneurons evoking a decline in anxiety-like behavior. Acute DOI enhances the firing activity of PV-positive interneurons within the vHpc CA1/sub region, which we show robustly express 5-HT_{2A} receptors. The anxiolytic actions of the serotonergic psychedelic DOI involve a key contribution of the 5-HT_{2A} receptors on PV-positive inhibitory interneurons in the vHpc CA1/sub region.

DISCUSSION

In this study, we present a series of experiments aimed at identifying the specific brain region, neuronal cell type, and receptor targeted by the serotonergic psychedelic DOI to regulate anxiety-like behavior in rats and mice. Our results collectively implicate PV-positive interneurons in the vHpc CA1/sub region as a central target for the anxiolytic actions of the serotonergic psychedelic DOI.

Reduction in anxiety-like behavior on the EPM following acute, systemic administration of DOI was observed in both male and female rats and mice, indicating that these DOI-evoked anxiolytic effects are robust across species and do not exhibit sex differences. Our findings agree with prior studies, which show that DOI elicits reduced anxiety-like behavioral responses on the EPM and elevated zero maze.[13] However, several studies also indicate differential effects of serotonergic psychedelics on anxiety-like behavior, with enhanced anxiety-like behavior evoked by acute DMT or psilocybin or chronic dosing with psilocin,[25–27] and contrasting reports of an amelioration of stress-induced anxiety-like behavior following chronic microdosing with LSD.[10] These findings highlight the importance of dose, strain, and stress history of the animal model when interpreting the impact of serotonergic psychedelics on anxiety-like behavioral responses.

To address whether DOI acts on a discrete brain region to exert its anxiolytic actions, we specifically targeted the key nodes of the limbic circuits implicated in regulating anxiety-like behavior.[28,29] Direct infusion of DOI into the vHpc CA1/sub region but not the dHpc CA1/sub region, mPFC subdivisions, or the BA resulted in reduced anxiety-like behavior on the EPM, phenocopying the anxiolytic effects of acute, systemic DOI treatment. Additionally, the systemic DOI-evoked change in total locomotion was not observed in our direct infusion studies with DOI targeting the "emotional triad" circuitry. It is noteworthy that we did not observe any change in HTR upon local DOI administration into the vHpc CA1/sub. These results further serve to highlight the recruitment of distinct neural circuits to mediate specific behavioral components of the effects of serotonergic psychedelics like DOI.

Our findings strongly indicate recruitment of vHpc CA1/sub region in mediating DOI-evoked anxiolysis. Prior reports suggest that the vHpc plays a significant role in regulating anxiety-like behavior. Cytotoxic and excitotoxic lesions of the vHpc can reduce anxiety-like behavior when assessed on conflict-anxiety maze tasks,[30,31] whereas exploration of "anxiogenic" open arms on the EPM is associated with enhanced theta rhythms in the vHpc.[32,33] However, the interconnected neural networks that modulate anxiety-like behavior are complex, and studies thus

(F) Fraction of neurons with increased or decreased firing rate following treatment with either vehicle or DOI. Red shading indicates time points where p value was <0.05 from binomial test, without correcting for multiple comparisons.
*$p < 0.05$. Data are mean ± SEM.
See also Figure S5.

Please cite this article in press as: Tiwari et al., Ventral hippocampal parvalbumin interneurons gate the acute anxiolytic action of the serotonergic psychedelic DOI, Neuron (2024), https://doi.org/10.1016/j.neuron.2024.08.016

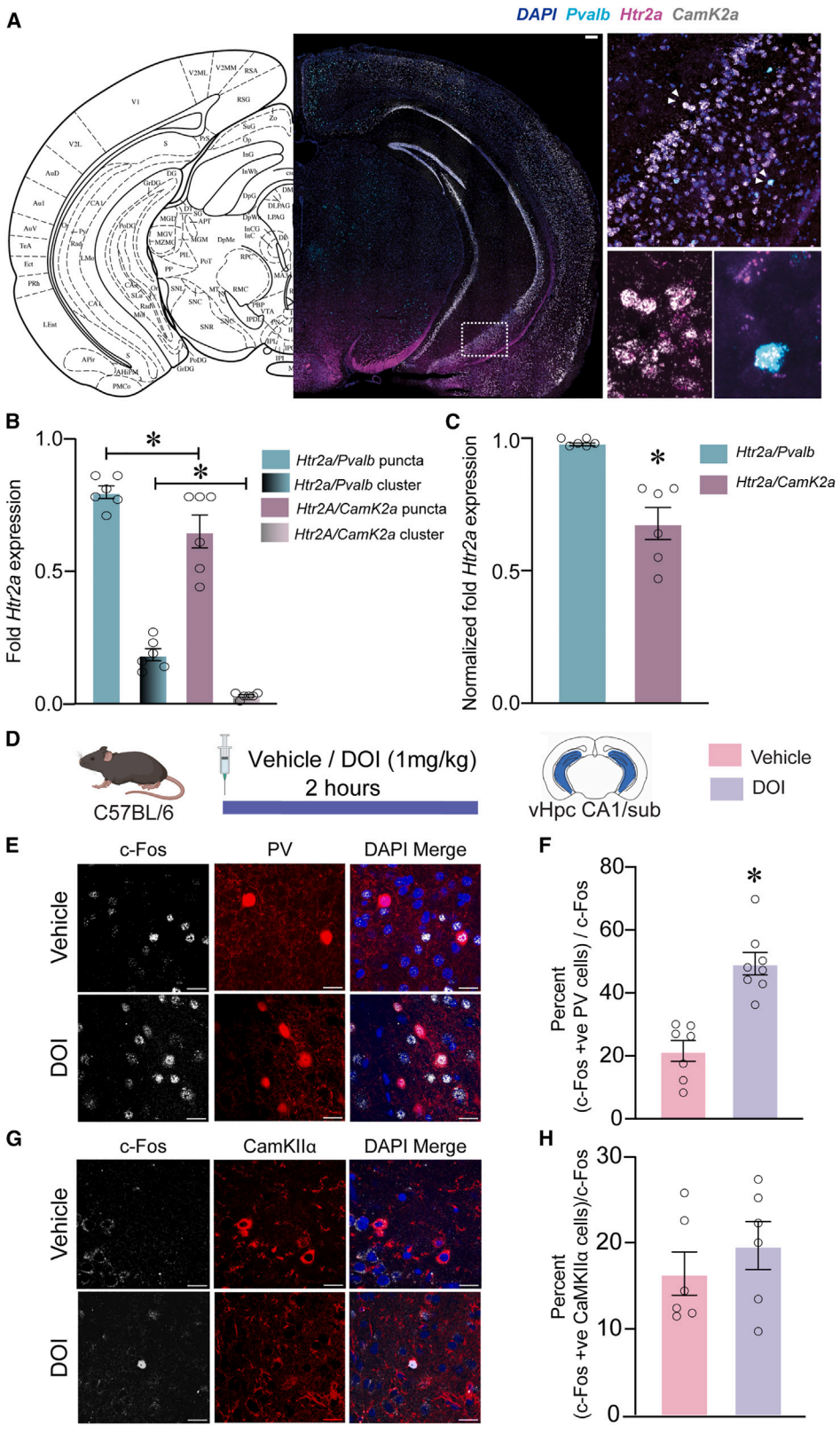

(legend on next page)

far have not been able to assign primacy to a single brain region in mediating the anxiolytic effects of serotonergic psychedelics like DOI. Our results reveal that the anxiolytic actions of acute, systemic DOI treatment on the EPM were completely prevented by selective pharmacological blockade of 5-HT_{2A} receptors in the vHpc CA1/sub region, highlighting both the critical importance of this brain region and the contribution of 5-HT_{2A} receptors.

Given that diverse serotonergic psychedelics exhibit a high affinity for multiple serotonin receptors, there remains a debate about the degree of contribution of 5-HT_{2A} receptors to the cellular and behavioral actions of specific serotonergic psychedelics.[34,35] Prior evidence suggests that the psilocybin-evoked cortical structural plasticity as well as the reversal of stress-evoked anhedonic responses are not blocked by pretreatment with the 5-$HT_{2A/C}$ receptor antagonist, ketanserin.[36,37] By contrast, ketanserin can block both the cortical structural plasticity and the decline in immobility on the forced swim test elicited by 5-MeO-DMT.[38] Furthermore, the effects of a single dose of DOI on fear-extinction and cortical neuronal structural plasticity are mediated via the 5-HT_{2A} receptor.[39,40] The action of tryptamine-derived serotonergic psychedelics like psilocybin and 5-MeO-DMT on stress-induced anhedonia also have been suggested to involve a key role for the 5-HT_{2A} receptor.[38] With regards to DOI, a potent 5-HT_{2A} partial agonist,[41,42] our results implicate a key role for 5-HT_{2A} receptors in the vHpc CA1/sub region in the anxiolytic actions of DOI. Our findings further indicated that restoration of 5-HT_{2A} receptor expression within neurons in the vHpc CA1/sub region of 5-HT_{2A}R loss-of-function mice could reinstate the DOI-evoked anxiolysis, which was otherwise absent in the 5-HT_{2A}RKO mouse line. In this regard, it is particularly interesting to compare our results to a prior report indicating that genetic restoration of 5-HT_{2A} receptors in the neocortex restores the HTR to both LSD and DOI.[43] This underscores the fact that specific behavioral features evoked by serotonergic psychedelics like DOI likely involve the contribution of discrete neural circuits, with 5-HT_{2A} receptors in the neocortex contributing to the HTR,[44] and 5-HT_{2A} receptors in the vHpc CA1/sub region mediating the anxiolytic responses as evidenced in our study.

While the impact of serotonergic psychedelics on neuronal activity within the neocortex has been the focus of several studies, with reports indicating heterogeneous effects of increased as well as decreased firing rates of cortical neurons,[45,46] there is a paucity of information on the effects of serotonergic psychedelics on the hippocampus.[47] Our electrophysiological analysis of single-unit recordings using neuropixels probes within the vHpc CA1/sub region indicates that DOI significantly enhances the firing rate of both FS and RS classes of neurons, albeit with a higher fraction of FS neurons exhibiting increased neuronal firing. FS neurons are predominantly PV-positive inhibitory interneurons,[48] that are known to be present in the vHpc CA1/sub region targeted in our study.[22,49–52] Our opto-tagging experiments confirm that acute DOI administration enhances the firing rate of PV-positive FS neurons in the vHpc CA1/sub region. Furthermore, RNAscope analysis indicates the robust expression of 5-HT_{2A} receptors on almost all PV-positive neurons in this region, which agrees with prior evidence that 5-HT_{2A} receptors are expressed by most GABAergic neurons in the vHpc.[53–55] However, it is interesting that our electrophysiological experiments suggest that the DOI-evoked increase in firing rate appears to be restricted to a subset of 5-HT_{2A} receptor expressing PV-positive neurons in the vHpc CA1/sub region. PV-positive neurons include different morphological subtypes,[56] for example, large, small, or nest basket cells, and chandelier cells, which can be further divided into additional subclasses based on molecular signatures.[57] The precise subclass of PV-positive neurons recruited by DOI remains unclear at present. Immunofluorescence analysis for the neuronal activity marker, c-Fos, also revealed that acute systemic DOI induced an increase in c-Fos/PV double-positive cells and not c-Fos/CamKIIα double-positive cells in the vHpc CA1/sub region. Our results raise the intriguing possibility that the anxiolytic actions of DOI may involve invoking an inhibitory tone in the vHpc via recruitment of PV-positive inhibitory interneurons.

Figure 5. PV-positive interneurons in the vHpc CA1/sub region primarily express 5-HT_{2A} receptors and exhibit DOI-evoked enhanced c-*fos* expression

(A) Left: shown is a representative confocal image of *in situ* hybridization for *Pvalb* (cyan), *Htr2a* (magenta), *CamK2a* (gray), and DAPI (blue) staining for nuclei. vHpc overview aligned to the brain atlas coordinates AP: −3.4, ML: ±3.0 mm, DV: −4.5 mm. Scale bar: 100 μm. Right, high-magnification images of the boxed area, showing *Pvalb*-positive cells and *CamK2a*-positive cells in the vHpc expressing *Htr2a*.

(B) Quantification showing the relative distribution of puncta and clusters of *Htr2a* in *Pvalb*-positive or *CamK2a*-positive cells ($F_{(3,20)}$ = 108.0) (*n* = 6 mice:3 males and 3 females).

(C) Quantification showing the overall level of co-expression of *Htr2a* with *Pvalb*-positive or *CamK2a*-positive cells ($F_{(5,5)}$ = 116.2) (*n* = 6 mice:3 males and 3 females).

(D) Shown is a schematic for the experimental paradigm to examine the influence of acute DOI treatment on the expression of the neuronal activation marker, c-Fos, in the vHpc CA1/sub region in C57BL/6 mice.

(E) Shown are representative images for immunohistochemical staining of c-Fos (first column; gray) staining in PV-positive neurons (middle column; red) and their colocalization (last column; DAPI: blue) in the vHpc CA1/sub region of vehicle (upper) and DOI-treated (bottom) cohorts.

(F) Mice subjected to systemic DOI treatment show a significant increase in the percent colocalization of the neuronal activation marker c-Fos with PV in the vHpc CA1/sub region as compared with their vehicle-treated controls ($F_{(7,6)}$ = 1.29; Veh:*n* = 7, DOI:*n* = 8).

(G) Shown are representative images for immunohistochemical staining of c-Fos (first column; gray) staining in CamKIIα-positive neurons (middle column; red) and their colocalization (last column; DAPI:blue) in the vHpc CA1/sub region of vehicle-treated (upper) and DOI-treated (bottom) cohorts.

(H) Mice subjected to systemic DOI treatment show no change in the percent colocalization of the neuronal activation marker c-Fos with CamKIIα in the vHpc CA1/sub region as compared with their vehicle-treated controls ($F_{(5,5)}$ = 1.22). (Veh:*n* = 6, DOI:*n* = 6).

*$p < 0.05$; t test (C, E, and F) or one-way ANOVA (B) followed by Tukey's multiple comparisons test. Hollow circles represent individual data points. Data are mean ± SEM.

See also Figure S6.

Please cite this article in press as: Tiwari et al., Ventral hippocampal parvalbumin interneurons gate the acute anxiolytic action of the serotonergic psychedelic DOI, Neuron (2024), https://doi.org/10.1016/j.neuron.2024.08.016

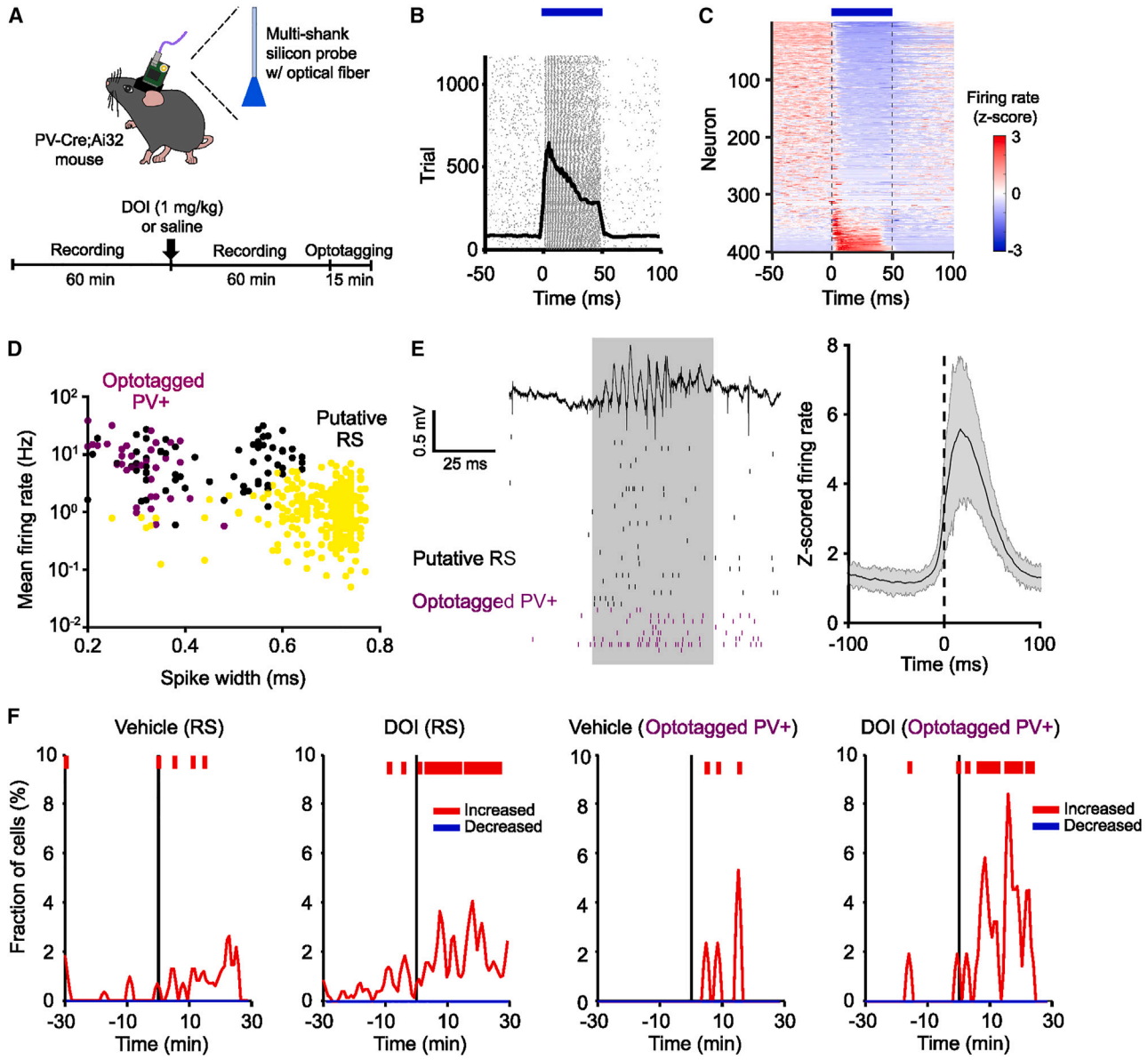

Figure 6. Acute systemic administration of DOI alters firing rates in optogenetically identified PV-positive cells in the ventral hippocampal CA1/sub region *in vivo*

(A) Schematic of chronic *in vivo* physiology recordings. Top: awake PV-Cre::ChR2 (PV-Cre;Ai32) mouse with chronically implanted multi-shank silicone probes. A 200 μm optical fiber was attached to the probe to enable optogenetic stimulation of PV-positive interneurons via 470 nm light. Bottom: timeline of experiment.

(B) Example response of an identified PV-positive interneuron to the 50 ms blue light pulse.

(C) Average *Z* scored firing rate of all units to the optogenetic stimulation, sorted by response intensity (n = 400 cells from 4 mice across 12 sessions).

(D) Comparison of single-cell average firing rate (Hz) with trough-to-peak spike width (ms) for optogenetically identified PV-positive cells (purple), putative pyramidal cells (yellow), and other neurons (gray), showing distinct clusters in spike properties.

(E) Left: example recording showing putative pyramidal neurons (black) and PV-positive interneurons (purple) firing during a hippocampal sharp-wave ripple event, the duration of which is designated by gray shading. Top: example LFP trace from the CA1 pyramidal layer of the hippocampus. Bottom: single spikes from individual neurons over the course of the event. Each row is an individual neuron, and each tick is a single spike. Note the sparse but distinct increase in firing in RS neurons (n = 30 cells in this window) compared with the strong, persistent firing of the opto-tagged PV+ interneurons (n = 8 cells in this window). Right: average *Z* scored firing rate response of PV-positive interneurons during hippocampal sharp-wave ripple events (n = 37 PV-positive interneurons).

(F) Fraction of neurons with increased or decreased firing rate following treatment with either vehicle or DOI. Red shading indicates time points with $p < 0.001$ from binomial test, without correcting for multiple comparisons (vehicle:n = 17 PV-positive cells and n = 121 RS cells from 3 mice across 5 vehicle-treatment sessions; DOI: n = 22 PV-positive cells and n = 171 RS cells from 4 mice across 7 DOI-treatment sessions). One of the 14 non-tagged FS interneurons responds to the DOI at the same magnitude of 5 standard deviations (Wilcoxon-rank test, $p < 0.05$, data not shown).

*$p < 0.05$. Circles represent individual cells (purple: opto-tagged PV-positive neurons; yellow: putative regular spiking neurons; gray: other unidentified neurons). Data are mean ± SEM.

Please cite this article in press as: Tiwari et al., Ventral hippocampal parvalbumin interneurons gate the acute anxiolytic action of the serotonergic psychedelic DOI, Neuron (2024), https://doi.org/10.1016/j.neuron.2024.08.016

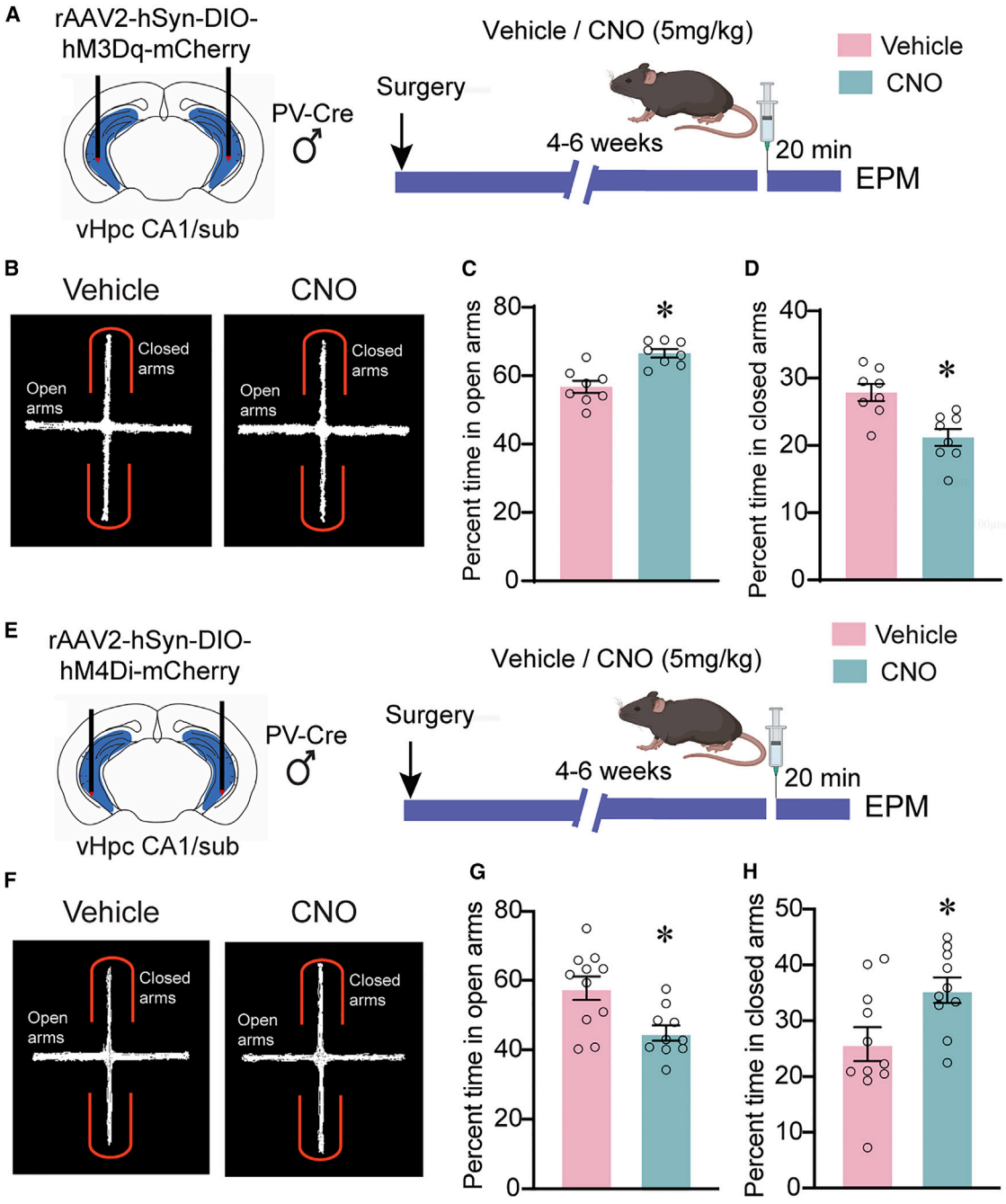

Figure 7. PV-positive inhibitory interneurons in the ventral hippocampal CA1/sub region regulate anxiety-like behavior on the EPM

(A) Shown is a schematic for the experimental paradigm to assess the effects of hM3Dq-DREADD-mediated chemogenetic activation of PV-positive inhibitory neurons in the vHpc CA1/sub region using rAAV2-hSyn-DIO-hM3Dq-mCherry virus expressed in PV-Cre animals. Animals were treated with vehicle or the DREADD ligand CNO (5 mg/kg) prior to behavioral analysis on the EPM.

(B) Shown are the tracks on the EPM for a representative vehicle (left) or CNO (right) administered PV-Cre mouse, expressing the hM3Dq-DREADD in PV-positive inhibitory neurons of the vHpc CA1/sub region.

(C and D) CNO-treated PV-Cre mice, expressing the hM3Dq-DREADD in PV-positive neurons of the vHpc CA1/sub region, show a significant increase in percent time in the open arms (G:$F_{(7,7)} = 2.09$) and a significant decrease in percent time in the closed arms (H:$F_{(7,7)} = 1.01$) (Veh:$n = 8$, CNO:$n = 8$).

(E) Shown is a schematic for the experimental paradigm to assess the effects of hM4Di-DREADD-mediated chemogenetic inhibition of PV-positive inhibitory neurons in the vHpc CA1/sub region using rAAV2-hSyn-DIO-hM4Di-mCherry virus expressed in PV-Cre animals. Animals were treated with vehicle or the DREADD ligand CNO (5 mg/kg) prior to behavioral analysis on the EPM.

(F) Shown are the tracks on the EPM for a representative vehicle (left) or CNO (right) administered PV-Cre mouse, expressing the hM4Di-DREADD in PV-positive inhibitory neurons of the vHpc CA1/sub region.

(legend continued on next page)

Please cite this article in press as: Tiwari et al., Ventral hippocampal parvalbumin interneurons gate the acute anxiolytic action of the serotonergic psychedelic DOI, Neuron (2024), https://doi.org/10.1016/j.neuron.2024.08.016

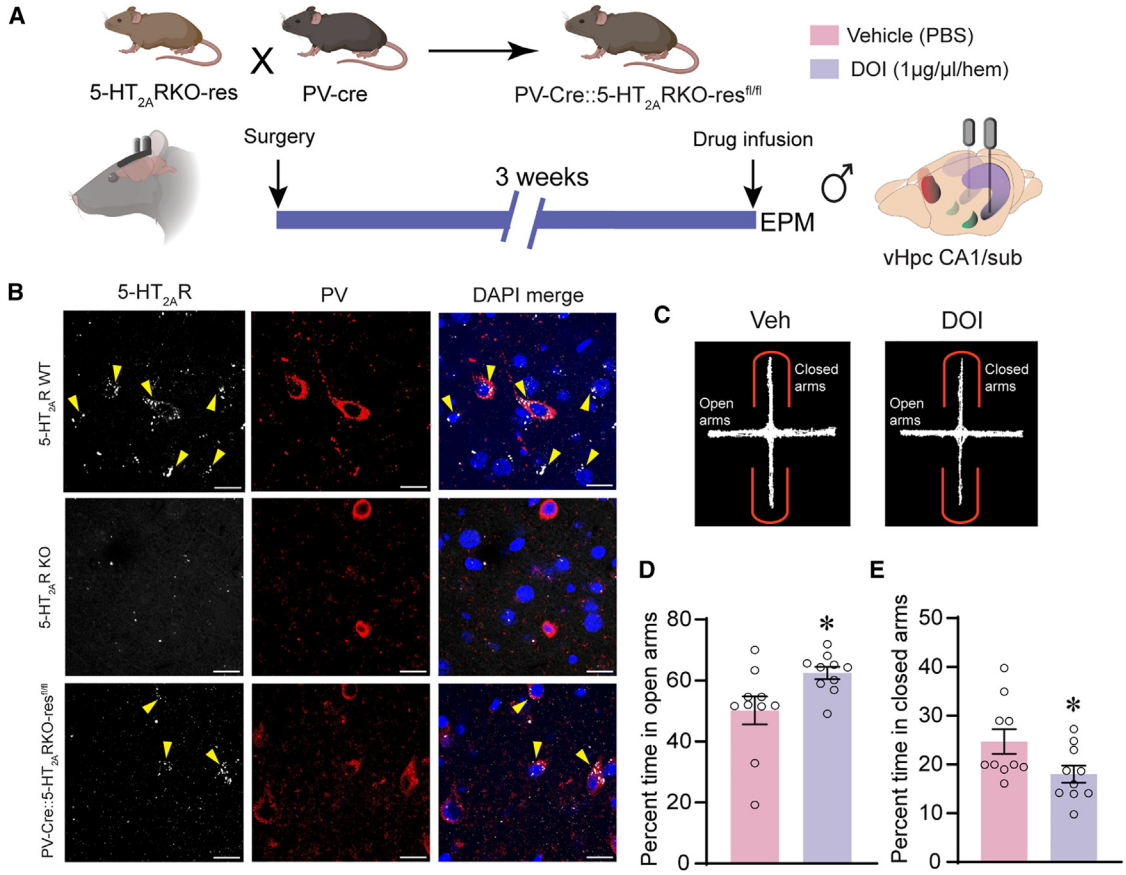

Figure 8. 5-HT$_{2A}$ receptors on PV-positive inhibitory interneurons in the ventral hippocampal CA1/sub region contribute to the DOI-evoked decline in anxiety-like behavior on the EPM

(A) Shown is a schematic for the breeding strategy (upper) for the generation of PV-Cre::5-HT$_{2A}$RKO-res$^{fl/fl}$ bigenic mouse line. The lower panel illustrates the experimental paradigm to address whether selective restoration of 5-HT$_{2A}$ receptors in PV-positive neurons in 5-HT$_{2A}$R KO background reinstates the decrease in anxiety-like behavior on the EPM noted with DOI infusion (1 μg/μL per hemisphere) in vHpc CA1/sub region.

(B) Shown are representative double immunofluorescence images indicating the colocalization of 5-HT$_{2A}$ receptors (first column; gray) with the marker PV (middle column; red) and a merge (last column; DAPI: blue) in the vHpc CA1/sub region of 5-HT$_{2A}$WT (upper), 5-HT$_{2A}$KO (middle), and PV-Cre::5-HT$_{2A}$RKO-res$^{fl/fl}$ bigenic (bottom) mouse lines (scale bar: 20 μm).

(C) Shown are the tracks on the EPM for a representative vehicle (left) or DOI (right) administered PV-Cre::5-HT$_{2A}$RKO-res$^{fl/fl}$ bigenic male mouse following direct infusion into the vHpc CA1/sub region.

(D and E) DOI-treated PV-Cre::5-HT$_{2A}$RKO-res$^{fl/fl}$ bigenic mice, with a selective restoration of 5-HT$_{2A}$ receptors in PV-positive neurons of the vHpc CA1/sub region, show a significant increase in percent time in the open arms (M:$F_{(9,9)}$ = 5.02) and a significant decrease in percent time in the closed arms (N:$F_{(9,9)}$ = 2.06) (Veh:n = 10, DOI:n = 10).

*p < 0.05. Hollow circles represent individual data points. Data are mean ± SEM.

See also Figure S8.

Prior studies have shown that chemogenetic inhibition of CamKIIα-positive projection neurons of the vHpc CA1/sub region exhibited a significant decline in anxiety-like behavioral responses on the EPM.[58–60] Similarly, prior evidence suggests a recruitment of inhibitory interneurons within the vHpc in conflict-based anxiety tasks.[61,62] The fraction of inhibitory interneurons increases across the dorso-ventral axis of the hippocampus, suggestive of a substantial impact of these neurons on gating activity and modulation of information processing within the vHpc.[63] A recent study showed that vHpc PV neurons activate upon entry into the open arms of the EPM, and optogenetically inhibiting these neurons can lead to persistent anxiety-like behavior.[64] Here, we provide evidence that hM3Dq-DREADD-mediated chemogenetic activation and hM4Di-DREADD-mediated inhibition of PV-positive inhibitory interneurons in the vHpc CA1/sub region evoke significant anxiolytic and anxiogenic effects in the EPM, respectively.

(G and H) CNO-treated PV-Cre mice, expressing the hM4Di-DREADD in PV-positive neurons of the vHpc CA1/sub region, show a significant decrease in percent time in the open arms (G:$F_{(10,9)}$ = 2.56) and a significant decrease in percent time in the closed arms (H:$F_{(10,9)}$ = 1.92) (Veh:n = 10, CNO:n = 11).

*p < 0.05. Hollow circles represent individual data points. Data are mean ± SEM.

See also Figure S7.

Please cite this article in press as: Tiwari et al., Ventral hippocampal parvalbumin interneurons gate the acute anxiolytic action of the serotonergic psychedelic DOI, Neuron (2024), https://doi.org/10.1016/j.neuron.2024.08.016

Given that acute systemic DOI treatment increases the firing rate of FS PV-positive inhibitory interneurons, this puts forth a possible hypothesis that DOI could recruit PV-positive inhibitory interneurons via its action on 5-HT_{2A} receptors to modulate anxiety-like behavior. A speculative possibility is that DOI administration via the recruitment of PV-positive interneurons in the vHpc CA1/sub region may enhance inhibitory tone in this neural circuit, which has previously been linked to anxiolytic responses on the EPM. Capitalizing on our 5-HT_{2A}RKO-res$^{fl/fl}$ mouse line, we selectively restored the expression of 5-HT_{2A} receptors on PV-positive interneurons using a bigenic PV-Cre::5-HT_{2A}RKO-res$^{fl/fl}$ mouse line, followed by direct infusion of DOI into the vHpc CA1/sub region. Unlike 5-HT_{2A}RKO mice, which do not exhibit any anxiolytic response to DOI infusion in the vHpc CA1/sub region, restoration of 5-HT_{2A} receptors on PV-positive interneurons is sufficient to evoke anxiolytic responses on the EPM following DOI administration into the vHpc CA1/sub region. By contrast, selectively restoring 5-HT_{2A} receptors in CamKIIα-positive neurons of the vHpc CA1/sub region did not influence DOI-evoked anxiolysis. These results indicate that the anxiolytic action of DOI involves a key role for 5-HT_{2A} receptor expressing PV-positive inhibitory interneurons within the vHpc CA1/sub region. Our work motivates future investigation into the contribution of other hippocampal regions, as well as specific downstream targets of the vHpc projections, that contribute to the regulation of anxiety-like behavior in response to serotonergic psychedelics.[28,29,32,33,58–60] It is likely that divergent projection streams and distinct neural circuits may differentially parcellate information processing relevant to specific components of approach-avoidance behavior under the effects of serotonergic psychedelics.

Clinical studies suggest that serotonergic psychedelics like LSD and psilocybin may be effective in treating anxiety disorders,[65–72] but the mechanism via which these compounds exert their effect on anxiety remains to be explored. Unlike most serotonergic psychedelics, which are reported to have high affinity for multiple serotonergic receptors, DOI exhibits preferential binding to the 5-HT_2 class of receptors, with a high affinity for the 5-HT_{2A} receptors. While DOI has been extensively used in studies with animal models, it has not been applied in a clinical context to the best of our knowledge. Hence, a direct extrapolation of our findings with DOI to other serotonergic psychedelics merits caution, given the possibility of a role for additional serotonergic receptors and the targeting of distinct neural circuits. Further, while our work points to potent anxiolytic actions of acute DOI administration, the longer-term consequences on anxiety-like behavior, the impact of sustained exposure to DOI, and the consequences of DOI treatment in animals with a stress history remain to be explored. Our work motivates future studies to dissect the anatomical underpinnings of the anxiolytic actions of diverse serotonergic psychedelics, as well as assessing their role in a wide spectrum of behavioral responses to effectively harness their therapeutic potential.

RESOURCE AVAILABILITY

Lead contact

Further information and requests for reagents may be directed to and will be fulfilled by the lead contact, Prof. Vidita A. Vaidya (vvaidya@tifr.res.in).

Materials availability

This study did not generate new unique reagents or mouse lines.

Data and code availability

- All data reported in this paper will be shared by the lead contact upon request.
- This paper does not report original code.
- Any additional information required to reanalyze the data reported in this paper is available from the lead contact upon request.

ACKNOWLEDGMENTS

The study was supported by project RTI4003 from the Department of Atomic Energy to Tata Institute of Fundamental Research and by the Sree Ramakrishna Paramahamsa Research Grant (2020) from the Sree Padmavathi Venkateswara Foundation (SreePVF), Vijayawada, Andhra Pradesh (V.A.V.); NIH/NIMH grants R01MH121848, R01MH128217, and R01MH137047 and One Mind—COMPASS Rising Star Award (A.C.K.); NIH/NIDA fellowship F30DA059437 and NIH/NIGMS medical scientist training grant T32GM007205 (P.A.D.); NIH grant R00MH120343, 1DP2MH136496, Sloan Fellowship, Whitehall Research Grant, and Klingenstein-Simons Fellowship (A.F.-R); NIH grants R01MH115049 and R01MH115914 (K.G.B.); NIH grant 5R01MH132911-02 (M.S.A.); Sackler Institute Award and NIH grant 1K01MH131895-01A1 (G.Z.); and the National Science Foundation Graduate Research Fellowship grant DGE-2139899 (L.A.K.).

We thank Dr. Balaganesh Janakiraman for assistance in generation of specific bigenic mouse strains. We thank the animal house staff at the TIFR, Yale University School of Medicine, Cornell University, and Columbia University for technical assistance. We thank K.V. Boby for assistance with confocal imaging at TIFR.

AUTHOR CONTRIBUTIONS

Conceptualization: P.T. and V.A.V.; methodology, investigation, and visualization: P.T., P.A.D., D.K., R.M.V., L.A.K., M.S., G.Z., A.B., P.R.C., A.P., S.S., A.F.-R., A.C.K., and V.A.V.; funding acquisition: V.A.V., A.C.K., A.F.-R., M.S.A., and K.G.B.; project administration: V.A.V.; supervision: V.A.V. and A.C.K., writing – original draft: P.T., P.A.D., A.C.K., and V.A.V.; writing – review and editing: P.T., P.A.D., L.A.K., G.Z., M.S.A., A.F.-R., A.C.K., and V.A.V.

DECLARATION OF INTERESTS

A.C.K. has been a scientific advisor or consultant for Boehringer Ingelheim, Empyrean *Neuroscience*, Freedom Biosciences, Biohaven Pharmaceuticals, and Psylo. A.C.K. has received research support from Intra-Cellular Therapies. These duties had no influence on the content of this article.

STAR★METHODS

Detailed methods are provided in the online version of this paper and include the following:

- KEY RESOURCES TABLE
- EXPERIMENTAL MODEL AND STUDY PARTICIPANT DETAILS
  - Animals
  - Viral constructs
- METHOD DETAILS
  - Drug treatment
  - Surgeries
  - Behavior assays
  - Electrophysiological recordings for neuropixels
  - Electrophysiological recordings for opto-tagging
  - RNAscope experiments
  - Immunohistochemical and histological analysis
  - Western blotting
- QUANTIFICATION AND STATISTICAL ANALYSIS

- Statistics for behavioral, immunofluorescence, and RNAscope assays
- Electrophysiological analysis for neuropixels recordings
- Spike sorting and single-unit classification for opto-tagging experiments
- Brain state detection
- Sharp wave ripple detection and spike content analysis
- Electrophysiological analysis for opto-tagging recordings

SUPPLEMENTAL INFORMATION

Supplemental information can be found online at https://doi.org/10.1016/j.neuron.2024.08.016.

Received: June 15, 2023
Revised: May 8, 2024
Accepted: August 27, 2024
Published: September 24, 2024

REFERENCES

1. Kelmendi, B., Kaye, A.P., Pittenger, C., and Kwan, A.C. (2022). Psychedelics. Curr. Biol. *32*, R63–R67. https://doi.org/10.1016/J.CUB.2021.12.009.
2. Nichols, D.E., Johnson, M.W., and Nichols, C.D. (2017). Psychedelics as Medicines: An Emerging New Paradigm. Clin. Pharmacol. Ther. *101*, 209–219. https://doi.org/10.1002/CPT.557.
3. Carhart-Harris, R.L., and Goodwin, G.M. (2017). The Therapeutic Potential of Psychedelic Drugs: Past, Present, and Future. Neuropsychopharmacology *42*, 2105–2113. https://doi.org/10.1038/NPP.2017.84.
4. Vollenweider, F.X., and Preller, K.H. (2020). Psychedelic drugs: neurobiology and potential for treatment of psychiatric disorders. Nat. Rev. Neurosci. *21*, 611–624. https://doi.org/10.1038/s41583-020-0367-2.
5. Vollenweider, F.X., Vollenweider-Scherpenhuyzen, M.F.I., Bäbler, A., Vogel, H., and Hell, D. (1998). Psilocybin induces schizophrenia-like psychosis in humans via a serotonin-2 agonist action. NeuroReport *9*, 3897–3902. https://doi.org/10.1097/00001756-199812010-00024.
6. Davis, A.K., Barrett, F.S., May, D.G., Cosimano, M.P., Sepeda, N.D., Johnson, M.W., Finan, P.H., and Griffiths, R.R. (2021). Effects of Psilocybin-Assisted Therapy on Major Depressive Disorder: A Randomized Clinical Trial. JAMA Psychiatry *78*, 1. https://doi.org/10.1001/JAMAPSYCHIATRY.2020.3285.
7. De Gregorio, D., Aguilar-Valles, A., Preller, K.H., Heifets, B.D., Hibicke, M., Mitchell, J., and Gobbi, G. (2021). Hallucinogens in Mental Health: Preclinical and Clinical Studies on LSD, Psilocybin, MDMA, and Ketamine. J. Neurosci. *41*, 891–900. https://doi.org/10.1523/JNEUROSCI.1659-20.2020.
8. Krediet, E., Bostoen, T., Breeksema, J., van Schagen, A., Passie, T., and Vermetten, E. (2020). Reviewing the Potential of Psychedelics for the Treatment of PTSD. Int. J. Neuropsychopharmacol. *23*, 385–400. https://doi.org/10.1093/IJNP/PYAA018.
9. Nichols, D.E., and Walter, H. (2021). The History of Psychedelics in Psychiatry. Pharmacopsychiatry *54*, 151–166. https://doi.org/10.1055/a-1310-3990.
10. De Gregorio, D., Inserra, A., Enns, J.P., Markopoulos, A., Pileggi, M., El Rahimy, Y., Lopez-Canul, M., Comai, S., and Gobbi, G. (2022). Repeated lysergic acid diethylamide (LSD) reverses stress-induced anxiety-like behavior, cortical synaptogenesis deficits and serotonergic neurotransmission decline. Neuropsychopharmacology *47*, 1188–1198. https://doi.org/10.1038/S41386-022-01301-9.
11. Hibicke, M., Landry, A.N., Kramer, H.M., Talman, Z.K., and Nichols, C.D. (2020). Psychedelics, but Not Ketamine, Produce Persistent Antidepressant-like Effects in a Rodent Experimental System for the Study of Depression. ACS Chem. Neurosci. *11*, 864–871. https://doi.org/10.1021/acschemneuro.9b00493.
12. Onaivi, E.S., Bishop-Robinson, C., Darmani, N.A., and Sanders-Bush, E. (1995). Behavioral effects of (±)-1-(2,5-dimethoxy-4-iodophenyl)-2-aminopropane. Life Sci. *57*, 2455–2466. https://doi.org/10.1016/0024-3205(95)02242-9.
13. Pędzich, B.D., Rubens, S., Sekssaoui, M., Pierre, A., Van Schuerbeek, A., Marin, P., Bockaert, J., Valjent, E., Bécamel, C., and De Bundel, D. (2022). Effects of a psychedelic 5-HT2A receptor agonist on anxiety-related behavior and fear processing in mice. Neuropsychopharmacology *47*, 1304–1314. https://doi.org/10.1038/S41386-022-01324-2.
14. Arvanov, V.L., Liang, X., Russo, A., and Wang, R.Y. (1999). LSD and DOB: Interaction with 5-HT2A receptors to inhibit NMDA receptor-mediated transmission in the rat prefrontal cortex. Eur. J. Neurosci. *11*, 3064–3072. https://doi.org/10.1046/j.1460-9568.1999.00726.x.
15. Marek, G.J., and Aghajanian, G.K. (1996). LSD and the phenethylamine hallucinogen DOI are potent partial agonists at 5-HT2A receptors on interneurons in rat piriform cortex. J. Pharmacol. Exp. Ther. *278*, 1373–1382.
16. Kwan, A.C., Olson, D.E., Preller, K.H., and Roth, B.L. (2022). The neural basis of psychedelic action. Nat. Neurosci. *25*, 1407–1419. https://doi.org/10.1038/S41593-022-01177-4.
17. Nichols, D.E. (2016). Psychedelics. Pharmacol. Rev. *68*, 264–355. https://doi.org/10.1124/pr.115.011478.
18. Weisstaub, N.V., Zhou, M., Lira, A., Lambe, E., González-Maeso, J., Hornung, J.P., Sibille, E., Underwood, M., Itohara, S., Dauer, W.T., et al. (2006). Cortical 5-HT2A receptor signaling modulates anxiety-like behaviors in mice. Science *313*, 536–540. https://doi.org/10.1126/SCIENCE.1123432/SUPPL_FILE/WEISSTAUB.SOM.PDF.
19. Jun, J.J., Steinmetz, N.A., Siegle, J.H., Denman, D.J., Bauza, M., Barbarits, B., Lee, A.K., Anastassiou, C.A., Andrei, A., Aydın, Ç., et al. (2017). Fully integrated silicon probes for high-density recording of neural activity. Nature *551*, 232–236. https://doi.org/10.1038/nature24636.
20. Mitchell, J.F., Sundberg, K.A., and Reynolds, J.H. (2007). Differential Attention-Dependent Response Modulation across Cell Classes in Macaque Visual Area V4. Neuron *55*, 131–141. https://doi.org/10.1016/j.neuron.2007.06.018.
21. Niell, C.M., and Stryker, M.P. (2008). Highly selective receptive fields in mouse visual cortex. J. Neurosci. *28*, 7520–7536. https://doi.org/10.1523/JNEUROSCI.0623-08.2008.
22. Bezaire, M.J., and Soltesz, I. (2013). Quantitative assessment of CA1 local circuits: knowledge base for interneuron-pyramidal cell connectivity. Hippocampus *23*, 751–785. https://doi.org/10.1002/HIPO.22141.
23. Jolly, S., Lang, V., Koelzer, V.H., Sala Frigerio, C., Magno, L., Salinas, P.C., Whiting, P., and Palomer, E. (2019). Single-Cell Quantification of mRNA Expression in The Human Brain. Sci. Rep. *9*, 12353. https://doi.org/10.1038/S41598-019-48787-W.
24. Puig, M.V., Ushimaru, M., and Kawaguchi, Y. (2008). Two distinct activity patterns of fast-spiking interneurons during neocortical UP states. Proc. Natl. Acad. Sci. USA *105*, 8428–8433. https://doi.org/10.1073/pnas.0712219105.
25. Cameron, L.P., Benson, C.J., Dunlap, L.E., and Olson, D.E. (2018). Effects of N, N-Dimethyltryptamine on Rat Behaviors Relevant to Anxiety and Depression. ACS Chem. Neurosci. *9*, 1582–1590. https://doi.org/10.1021/acschemneuro.8b00134.
26. Horsley, R.R., Páleníček, T., Kolin, J., and Valeš, K. (2018). Psilocin and ketamine microdosing: Effects of subchronic intermittent microdoses in the elevated plus-maze in male Wistar rats. Behav. Pharmacol. *29*, 530–536. https://doi.org/10.1097/FBP.0000000000000394.
27. Harari, R., Chatterjee, I., Getselter, D., and Elliott, E. (2024). Psilocybin induces acute anxiety and changes in amygdalar phosphopeptides independently from the 5-HT2A receptor. iScience *27*, 109686. https://doi.org/10.1016/j.isci.2024.109686.
28. Calhoon, G.G., and Tye, K.M. (2015). Resolving the neural circuits of anxiety. Nat. Neurosci. *18*, 1394–1404. https://doi.org/10.1038/nn.4101.

29. Tovote, P., Fadok, J.P., and Lüthi, A. (2015). Neuronal circuits for fear and anxiety. Nat. Rev. Neurosci. *16*, 317–331. https://doi.org/10.1038/nrn3945.

30. Bertagna, N.B., dos Santos, P.G.C., Queiroz, R.M., Fernandes, G.J.D., Cruz, F.C., and Miguel, T.T. (2021). Involvement of the ventral, but not dorsal, hippocampus in anxiety-like behaviors in mice exposed to the elevated plus maze: participation of CRF1 receptor and PKA pathway. Pharmacol. Rep. *73*, 57–72. https://doi.org/10.1007/s43440-020-00182-3.

31. Wang, C., Zhang, Y., Shao, S., Cui, S., Wan, Y., and Yi, M. (2019). Ventral Hippocampus Modulates Anxiety-Like Behavior in Male But Not Female C57BL/6 J Mice. Neuroscience *418*, 50–58. https://doi.org/10.1016/j.neuroscience.2019.08.032.

32. Adhikari, A., Topiwala, M.A., and Gordon, J.A. (2010). Synchronized activity between the ventral hippocampus and the medial prefrontal cortex during anxiety. Neuron *65*, 257–269. https://doi.org/10.1016/J.NEURON.2009.12.002.

33. Adhikari, A., Topiwala, M.A., and Gordon, J.A. (2011). Single units in the medial prefrontal cortex with anxiety-related firing patterns are preferentially influenced by ventral hippocampal activity. Neuron *71*, 898–910. https://doi.org/10.1016/j.neuron.2011.07.027.

34. Halberstadt, A.L., and Geyer, M.A. (2011). Multiple receptors contribute to the behavioral effects of indoleamine hallucinogens. Neuropharmacology *61*, 364–381. https://doi.org/10.1016/J.NEUROPHARM.2011.01.017.

35. De La Fuente Revenga, M., Jaster, A.M., McGinn, J., Silva, G., Saha, S., and González-Maeso, J. (2022). Tolerance and Cross-Tolerance among Psychedelic and Nonpsychedelic 5-HT2AReceptor Agonists in Mice. ACS Chem. Neurosci. *13*, 2436–2448. https://doi.org/10.1021/acschemneuro.2c00170.

36. Hesselgrave, N., Troppoli, T.A., Wulff, A.B., Cole, A.B., and Thompson, S.M. (2021). Harnessing psilocybin: antidepressant-like behavioral and synaptic actions of psilocybin are independent of 5-HT2R activation in mice. Proc. Natl. Acad. Sci. USA *118*, e2022489118. https://doi.org/10.1073/PNAS.2022489118.

37. Shao, L.X., Liao, C., Gregg, I., Davoudian, P.A., Savalia, N.K., Delagarza, K., and Kwan, A.C. (2021). Psilocybin induces rapid and persistent growth of dendritic spines in frontal cortex in vivo. Neuron *109*, 2535–2544.e4. https://doi.org/10.1016/J.NEURON.2021.06.008.

38. Cameron, L.P., Patel, S.D., Vargas, M.V., Barragan, E.V., Saeger, H.N., Warren, H.T., Chow, W.L., Gray, J.A., and Olson, D.E. (2023). 5-HT2ARs Mediate Therapeutic Behavioral Effects of Psychedelic Tryptamines. ACS Chem. Neurosci. *14*, 351–358. https://doi.org/10.1021/ACSCHEMNEURO.2C00718.

39. de la Fuente Revenga, M., Zhu, B., Guevara, C.A., Naler, L.B., Saunders, J.M., Zhou, Z., Toneatti, R., Sierra, S., Wolstenholme, J.T., Beardsley, P.M., et al. (2021). Prolonged epigenomic and synaptic plasticity alterations following single exposure to a psychedelic in mice. Cell Rep. *37*, 109836. https://doi.org/10.1016/J.CELREP.2021.109836.

40. Vargas, M.V., Dunlap, L.E., Dong, C., Carter, S.J., Tombari, R.J., Jami, S.A., Cameron, L.P., Patel, S.D., Hennessey, J.J., Saeger, H.N., et al. (2023). Psychedelics promote neuroplasticity through the activation of intracellular 5-HT2A receptors. Science *379*, 700–706. https://doi.org/10.1126/SCIENCE.ADF0435.

41. Fantegrossi, W.E., Murnane, K.S., and Reissig, C.J. (2008). The behavioral pharmacology of hallucinogens. Biochem. Pharmacol. *75*, 17–33. https://doi.org/10.1016/J.BCP.2007.07.018.

42. McKenna, D.J., and Peroutka, S.J. (1989). Differentiation of 5-hydroxytryptamine2 receptor subtypes using 125I-R-(-)2,5-dimethoxy-4-iodo-phenylisopropylamine and 3H-ketanserin. J. Neurosci. *9*, 3482–3490. https://doi.org/10.1523/JNEUROSCI.09-10-03482.1989.

43. González-Maeso, J., Weisstaub, N.V., Zhou, M., Chan, P., Ivic, L., Ang, R., Lira, A., Bradley-Moore, M., Ge, Y., Zhou, Q., et al. (2007). Hallucinogens recruit specific cortical 5-HT(2A) receptor-mediated signaling pathways to affect behavior. Neuron *53*, 439–452. https://doi.org/10.1016/J.NEURON.2007.01.008.

44. Canal, C.E., and Morgan, D. (2012). Head-twitch response in rodents induced by the hallucinogen 2,5-dimethoxy-4-iodoamphetamine: a comprehensive history, a re-evaluation of mechanisms, and its utility as a model. Drug Test. Anal. *4*, 556–576. https://doi.org/10.1002/DTA.1333.

45. Michaiel, A.M., Parker, P.R.L., and Niell, C.M. (2019). A Hallucinogenic Serotonin-2A Receptor Agonist Reduces Visual Response Gain and Alters Temporal Dynamics in Mouse V1. Cell Rep. *26*, 3475–3483.e4. https://doi.org/10.1016/J.CELREP.2019.02.104.

46. Wood, J., Kim, Y., and Moghaddam, B. (2012). Disruption of prefrontal cortex large scale neuronal activity by different classes of psychotomimetic drugs. J. Neurosci. *32*, 3022–3031. https://doi.org/10.1523/JNEUROSCI.6377-11.2012.

47. Domenico, C., Haggerty, D., Mou, X., and Ji, D. (2021). LSD degrades hippocampal spatial representations and suppresses hippocampal-visual cortical interactions. Cell Rep. *36*, 109714. https://doi.org/10.1016/J.CELREP.2021.109714.

48. Kawaguchi, Y., Katsumaru, H., Kosaka, T., Heizmann, C.W., and Hama, K. (1987). Fast spiking cells in rat hippocampus (CA1 region) contain the calcium-binding protein parvalbumin. Brain Res. *416*, 369–374. https://doi.org/10.1016/0006-8993(87)90921-8.

49. Hu, H., Gan, J., and Jonas, P. (2014). Interneurons. Fast-spiking, parvalbumin^{+} GABAergic interneurons: from cellular design to microcircuit function. Science *345*, 1255263. https://doi.org/10.1126/SCIENCE.1255263.

50. Pelkey, K.A., Chittajallu, R., Craig, M.T., Tricoire, L., Wester, J.C., and McBain, C.J. (2017). Hippocampal GABAergic Inhibitory Interneurons. Physiol. Rev. *97*, 1619–1747. https://doi.org/10.1152/PHYSREV.00007.2017.

51. Sun, Y., Nguyen, A.Q., Nguyen, J.P., Le, L., Saur, D., Choi, J., Callaway, E.M., and Xu, X. (2014). Cell-type-specific circuit connectivity of hippocampal CA1 revealed through Cre-dependent rabies tracing. Cell Rep. *7*, 269–280. https://doi.org/10.1016/J.CELREP.2014.02.030.

52. Udakis, M., Pedrosa, V., Chamberlain, S.E.L., Clopath, C., and Mellor, J.R. (2020). Interneuron-specific plasticity at parvalbumin and somatostatin inhibitory synapses onto CA1 pyramidal neurons shapes hippocampal output. Nat. Commun. *11*, 4395. https://doi.org/10.1038/s41467-020-18074-8.

53. Bombardi, C. (2012). Neuronal localization of 5-HT2A receptor immunoreactivity in the rat hippocampal region. Brain Res. Bull. *87*, 259–273. https://doi.org/10.1016/J.BRAINRESBULL.2011.11.006.

54. Bombardi, C., and Di Giovanni, G. (2013). Functional anatomy of 5-HT2A receptors in the amygdala and hippocampal complex: Relevance to memory functions. Exp. Brain Res. *230*, 427–439. https://doi.org/10.1007/s00221-013-3512-6.

55. Tanaka, K.F., Samuels, B.A., and Hen, R. (2012). Serotonin receptor expression along the dorsal-ventral axis of mouse hippocampus. Philos. Trans. R. Soc. Lond. B Biol. Sci. *367*, 2395–2401. https://doi.org/10.1098/RSTB.2012.0038.

56. Markram, H., Toledo-Rodriguez, M., Wang, Y., Gupta, A., Silberberg, G., and Wu, C. (2004). Interneurons of the neocortical inhibitory system. Nat. Rev. Neurosci. *5*, 793–807. https://doi.org/10.1038/nrn1519.

57. Tasic, B., Yao, Z., Graybuck, L.T., Smith, K.A., Nguyen, T.N., Bertagnolli, D., Goldy, J., Garren, E., Economo, M.N., Viswanathan, S., et al. (2018). Shared and distinct transcriptomic cell types across neocortical areas. Nature *563*, 72–78. https://doi.org/10.1038/s41586-018-0654-5.

58. Jimenez, J.C., Su, K., Goldberg, A.R., Paninski, L., Hen, R., and Kheirbek, M.A. (2018). Anxiety Cells in a Hippocampal-Hypothalamic Circuit Correspondence. Neuron *97*, 670–683.e6. https://doi.org/10.1016/j.neuron.2018.01.016.

59. Padilla-Coreano, N., Bolkan, S.S., Pierce, G.M., Blackman, D.R., Hardin, W.D., Garcia-Garcia, A.L., Spellman, T.J., and Gordon, J.A. (2016). Direct Ventral Hippocampal-Prefrontal Input Is Required for Anxiety-Related

Neural Activity and Behavior. Neuron *89*, 857–866. https://doi.org/10.1016/j.neuron.2016.01.011.

60. Parfitt, G.M., Nguyen, R., Bang, J.Y., Aqrabawi, A.J., Tran, M.M., Seo, D.K., Richards, B.A., and Kim, J.C. (2017). Bidirectional Control of Anxiety-Related Behaviors in Mice: Role of Inputs Arising from the Ventral Hippocampus to the Lateral Septum and Medial Prefrontal Cortex. Neuropsychopharmacology *42*, 1715–1728. https://doi.org/10.1038/NPP.2017.56.
61. Forro, T., Volitaki, E., Malagon-Vina, H., Klausberger, T., Nevian, T., and Ciocchi, S. (2022). Anxiety-related activity of ventral hippocampal interneurons. Prog. Neurobiol. *219*, 102368. https://doi.org/10.1016/J.PNEUROBIO.2022.102368.
62. Li, H., Zhao, J., Lai, L., Xia, Y., Wan, C., Wei, S., Liang, J., Chen, Y., and Xu, N. (2022). Loss of SST and PV positive interneurons in the ventral hippocampus results in anxiety-like behavior in 5xFAD mice. Neurobiol. Aging *117*, 165–178. https://doi.org/10.1016/J.NEUROBIOLAGING.2022.05.013.
63. Jinno, S., and Kosaka, T. (2006). Cellular architecture of the mouse hippocampus: A quantitative aspect of chemically defined GABAergic neurons with stereology. Neurosci. Res. *56*, 229–245. https://doi.org/10.1016/j.neures.2006.07.007.
64. Volitaki, E., Forro, T., Li, K., Nevian, T., and Ciocchi, S. (2024). Activity of ventral hippocampal parvalbumin interneurons during anxiety. Cell Rep. *43*, 114295. https://doi.org/10.1016/j.celrep.2024.114295.
65. Gasser, P., Holstein, D., Michel, Y., Doblin, R., Yazar-Klosinski, B., Passie, T., and Brenneisen, R. (2014). Safety and efficacy of lysergic acid diethylamide-assisted psychotherapy for anxiety associated with life-threatening diseases. J. Nerv. Ment. Dis. *202*, 513–520. https://doi.org/10.1097/NMD.0000000000000113.
66. Holze, F., Gasser, P., Müller, F., Dolder, P.C., and Liechti, M.E. (2023). Lysergic Acid Diethylamide–Assisted Therapy in Patients With Anxiety With and Without a Life-Threatening Illness: A Randomized, Double-Blind, Placebo-Controlled Phase II Study. Biol. Psychiatry *93*, 215–223. https://doi.org/10.1016/j.biopsych.2022.08.025.
67. Griffiths, R.R., Johnson, M.W., Carducci, M.A., Umbricht, A., Richards, W.A., Richards, B.D., Cosimano, M.P., and Klinedinst, M.A. (2016). Psilocybin produces substantial and sustained decreases in depression and anxiety in patients with life-threatening cancer: A randomized double-blind trial. J. Psychopharmacol. *30*, 1181–1197. https://doi.org/10.1177/0269881116675513.
68. Grob, C.S., Danforth, A.L., Chopra, G.S., Hagerty, M., McKay, C.R., Halberstadt, A.L., and Greer, G.R. (2011). Pilot study of psilocybin treatment for anxiety in patients with advanced-stage cancer. Arch. Gen. Psychiatry *68*, 71–78. https://doi.org/10.1001/archgenpsychiatry.2010.116.
69. Grof, S., Goodman, L.E., Richards, W.A., and Kurland, A.A. (1973). LSD assisted psychotherapy in patients with terminal cancer. Int. Pharmacopsychiatry *8*, 129–144. https://doi.org/10.1159/000467984.
70. King, F., and Hammond, R. (2021). Psychedelics as Reemerging Treatments for Anxiety Disorders: Possibilities and Challenges in a Nascent Field. Focus (Am Psychiatr. Publ) *19*, 190–196. https://doi.org/10.1176/appi.focus.20200047.
71. Pahnke, W.N., Kurland, A.A., Goodman, L.E., and Richards, W.A. (1969). LSD-assisted psychotherapy with terminal cancer patients. Curr. Psychiatr. Ther. *9*, 144–152.
72. Ross, S., Bossis, A., Guss, J., Agin-Liebes, G., Malone, T., Cohen, B., Mennenga, S.E., Belser, A., Kalliontzi, K., Babb, J., et al. (2016). Rapid and sustained symptom reduction following psilocybin treatment for anxiety and depression in patients with life-threatening cancer: A randomized controlled trial. J. Psychopharmacol. *30*, 1165–1180. https://doi.org/10.1177/0269881116675512.
73. Oliva, A., Fernández-Ruiz, A., Leroy, F., and Siegelbaum, S.A. (2020). Hippocampal CA2 sharp-wave ripples reactivate and promote social memory. Nature *587*, 264–269. https://doi.org/10.1038/S41586-020-2758-Y.
74. Shamash, P., Carandini, M., Harris, K., and Steinmetz, N. (2018). A tool for analyzing electrode tracks from slice histology. Preprint at bioRxiv, 447995. https://doi.org/10.1101/447995.
75. Wang, Q., Ding, S.L., Li, Y., Royall, J., Feng, D., Lesnar, P., Graddis, N., Naeemi, M., Facer, B., Ho, A., et al. (2020). The Allen Mouse Brain Common Coordinate Framework: A 3D Reference Atlas. Cell *181*, 936–953.e20. https://doi.org/10.1016/J.CELL.2020.04.007.
76. Claudi, F., Tyson, A.L., Petrucco, L., Margrie, T.W., Portugues, R., and Branco, T. (2021). Visualizing anatomically registered data with brainrender. eLife *10*, e65751. https://doi.org/10.7554/eLife.65751.
77. Jia, X., Siegle, J.H., Bennett, C., Gale, S.D., Denman, D.J., Koch, C., and Olsen, S.R. (2019). High-density extracellular probes reveal dendritic backpropagation and facilitate neuron classification. J. Neurophysiol. *121*, 1831–1847. https://doi.org/10.1152/jn.00680.2018.
78. Pachitariu, M., Steinmetz, N.A., Kadir, S.N., Carandini, M., and Harris, K.D. (2016). Fast and accurate spike sorting of high-channel count probes with KiloSort. Adv. Neural Inf. Process. Syst. *29*, 4455–4463.
79. Petersen, P.C., Siegle, J.H., Steinmetz, N.A., Mahallati, S., and Buzsáki, G. (2021). CellExplorer: A framework for visualizing and characterizing single neurons. Neuron *109*, 3594–3608.e2. https://doi.org/10.1016/J.NEURON.2021.09.002.
80. Harvey, R.E., Robinson, H.L., Liu, C., Oliva, A., and Fernandez-Ruiz, A. (2023). Hippocampo-cortical circuits for selective memory encoding, routing, and replay. Neuron *111*, 2076–2090.e9. https://doi.org/10.1016/j.neuron.2023.04.015.
81. Liu, C., Todorova, R., Tang, W., Oliva, A., and Fernandez-Ruiz, A. (2023). Associative and predictive hippocampal codes support memory-guided behaviors. Science *382*, eadi8237. https://doi.org/10.1126/science.adi8237.
82. Sirota, A., Montgomery, S., Fujisawa, S., Isomura, Y., Zugaro, M., and Buzsáki, G. (2008). Entrainment of neocortical neurons and gamma oscillations by the hippocampal theta rhythm. Neuron *60*, 683–697. https://doi.org/10.1016/J.NEURON.2008.09.014.
83. Schomburg, E.W., Fernández-Ruiz, A., Mizuseki, K., Berényi, A., Anastassiou, C.A., Koch, C., and Buzsáki, G. (2014). Theta Phase Segregation of Input-Specific Gamma Patterns in Entorhinal-Hippocampal Networks. Neuron *84*, 470–485. https://doi.org/10.1016/j.neuron.2014.08.051.

Please cite this article in press as: Tiwari et al., Ventral hippocampal parvalbumin interneurons gate the acute anxiolytic action of the serotonergic psychedelic DOI, Neuron (2024), https://doi.org/10.1016/j.neuron.2024.08.016

STAR★METHODS

KEY RESOURCES TABLE

REAGENT or RESOURCE	SOURCE	IDENTIFIER
Antibodies		
mouse anti-CamKIIα	Cell Signaling Technologies	Cat # 50049; RRID:AB_2721906
mouse anti-PV	Sigma-Aldrich	Cat# P3088; RRID: AB_477329
rabbit anti-c-Fos	Cell Signaling Technologies	Cat# 2250; RRID: AB_2247211
rabbit anti-5-HT_{2A}R (for IHCs)	Neuromics	Cat # RA24288; RRID: AB_2122436
rabbit anti-5-HT_{2A}R (for WB)	Sigma-Aldrich: Calbiochem	Cat # PC176
rabbit anti-ß-actin	Abclonal	Cat # AC026; RRID: AB_2768234
HRP-conjugated Goat anti-Rabbit IgG	Abclonal	Cat # AS104
donkey anti-mouse Alexa Fluor 555	Invitrogen	Cat# A-31570
donkey anti-rabbit Alexa Fluor 488	Invitrogen	Cat# A-21206
donkey anti-mouse Alexa Fluor 488	Invitrogen	Cat# A-21202
donkey anti-rabbit Alexa Fluor 555	Invitrogen	Cat# A-31572
RNAscope probes		
Mm-Htr2a-C2	Advanced Cell Diagnostics	401291-C2
Mm-Camk2a-C3	Advanced Cell Diagnostics	445231-C3
Mm-Pvalb-C1	Advanced Cell Diagnostics	421931-C1
Virus		
rAAV2-hsyn-DIO-hM3Dq-mCherry	UNC Vector Core	N/A
rAAV2-hsyn-DIO-hM4Di-mCherry	UNC Vector Core	N/A
AAV9-Syn-Cre-GFP	SignaGen Lab	SL100892
AAV9-CamKII-HI-GFP-Cre.WPRE.SV40	Addgene	105551
rAAV2-hsyn-DIO-mCherry	UNC Vector Core	N/A
Drugs		
DOI	Sigma-Aldrich	42203-78-1
MDL100907	Tocris	4173
Clozapine-N-Oxide (CNO)	Tocris	‘4936
Experimental models: Organisms/strains		
C57BL/6	Jackson Laboratories, USA	Jax Strain 00064, 005304
PV-Cre (B6.129P2-Pvalbtm1(cre)Arbr/J)	Jackson Laboratories, USA	Jax Strain 008069
Ai32(RCL-ChR2(H134R)/EYFP)	Jackson Laboratories, USA	Jax Strain 012569
5-HT_{2A}RKO and WT (129S6/SvEv)	N/A	Kind gift from Prof. Jay Gingrich, Columbia University
PV-Cre::5-HT_{2A}RKO-res$^{fl/fl}$	Jackson Laboratories, USA and kind gift from Prof. Jay Gingrich, Columbia University	Generated at TIFR animal facility

EXPERIMENTAL MODEL AND STUDY PARTICIPANT DETAILS

Animals

Adult Sprague-Dawley rats, C57BL/6 (Jax Strain 00064, 005304; Jackson Laboratories, USA) mice were used for experiments. For transgenic mouse experiments, the mouse lines used were the 5-HT_{2A} receptor loss-of-function (5-HT_{2A}RKO, kind gift from Prof. Jay Gingrich), the PV-Cre (B6.129P2-Pvalbtm1(cre)Arbr/J; Jax Strain 008069; Jackson Laboratories), and Ai32:ChR2 (RCL-ChR2(H134R)/EYFP); Jax Strain 012569; Jackson Laboratories). The 5-HT_{2A}RKO line has a neo-stop cassette flanked by unidirectional lox P sites upstream to the *htr2a* gene facilitating the selective restoration of 5-HT_{2A} receptors based on the conditional expression of the Cre-recombinase. To generate the PV-Cre::5-HT_{2A}RKO-res$^{fl/fl}$ bigenic mouse line, male 5-HT_{2A}RKO mice were mated with female PV-Cre mice, and bigenic adult mice were used for specific experiments. PV-Cre::5-HT_{2A}RKO-res$^{fl/fl}$ bigenic adult mice have a selective restoration of 5-HT_{2A} receptors in PV-positive neurons, in a 5-HT_{2A} receptor loss-of-function background. For

opto-tagging experiments, we generated PV-Cre::ChR2 bigenic mice by crossing PV-Cre mice to Ai32 homozygous mice that encode ChR2 in a Cre-dependent manner.

All animals were maintained in the institutional animal house facility on a 12 hour light-dark cycle (7 am-7 pm) with *ad libitum* access to food and water. Experimental procedures were carried out as per the guidelines of the Committee for Control and Supervision of Experiments on Animals (CCSEA), Government of India and were approved by the Tata Institute of Fundamental Research (TIFR) animal ethics committee. Electrophysiology, opto-tagging and RNAscope experiments were carried out as per the guidelines by National Institutes of Health (NIH) Guide for Care and Use of Laboratory Animals and were approved by the Institutional Animal Care & Use Committee (IACUC) at Yale University, Cornell University and Columbia University respectively. Care was taken across all experiments to minimize any pain or suffering, and to restrict the number of animals used.

Viral constructs

For virus infusion experiments, AAV2-hsyn-DIO-hM3Dq-mCherry (Titer value (TV): 5.1x 10^{12} viral genomes per ml (vg/ml)), AAV2-hsyn-DIO-hM4Di-mCherry (TV: 4.6 x 10^{12} vg/ml), AAV9-CamKII-GFP-Cre (TV: 4.4 x 10^{12} vg/ml), AAV9-Syn-Cre-GFP (TV: 2.11x10^{12} vg/ml) and AAV2-hsyn-DIO-mCherry (TV: 3.1 x 10^{12} vg/ml) were used to target the vHpc CA1/sub region as per the experimental design.

METHOD DETAILS

Drug treatment

For systemic experiments, animals received intraperitoneal (*i.p.*) injections of vehicle (0.9% saline) or DOI (Cat. No. 42203-78-1, Sigma-Aldrich, USA). For stereotactic drug delivery, animals received vehicle (phosphate buffered saline - PBS), DOI (1μg/μl per hemisphere) or MDL100907 (1μg/μl per hemisphere) (Cat. No. 4173, Tocris, UK) through pre-implanted cannulas. For chemogenetic experiments, animals received *i.p*. Injections of vehicle (1% DMSO in 0.9% saline), or the DREADD ligand clozapine-N-oxide (CNO, 5 mg/kg) (Cat. No. 4936, Tocris, UK).

Surgeries

Stereotactic targets

Animals were first anesthetized with 3%–4% isoflurane in oxygen, and then maintained at 1%–2% isoflurane in oxygen throughout the surgical procedure. Using a stereotactic apparatus (Stoelting Co., USA), the animals were subjected to neurosurgeries for cannula implant placement and/or viral infusions. Using the bregma point as a reference, stereotactic coordinates for rat surgeries were as follows - ventral hippocampus (vHpc): AP – 5.5 mm, ML ± 5.0 mm, DV – 7.5 mm; dorsal hippocampus (dHpc): AP – 3.6 mm, ML ± 1.5 mm, DV – 2.6 mm; prelimbic cortex (PrL): AP +2.7 mm, ML ± 0.6 mm, DV – 4.0 mm; Infralimbic cortex (IL): AP + 3.2 mm, ML ± 0.6 mm, DV – 5.0 mm; and basal amygdala (BA): AP – 2.8 mm, ML ± 4.9 mm, DV – 8.4 mm. Stereotactic coordinates for mouse surgeries were as follows - vHpc: AP – 3.2 mm, ML ± 3.0 mm, DV – 4.5 mm. All animals were administered 200 μg/kg meloxicam (Melonex, Intas Pharmaceuticals, India) as a postoperative analgesic.

Cannula placement and viral delivery surgeries

Under the influence of general anesthesia, animals were subjected to stereotactic surgeries. The hair on the head was shaved and the scalp was cleaned using betadine before an incision was made to access the skull. Using the stereotactic coordinates, target areas were marked on the skull, and a 0.5 mm craniotomy was made using a dental drill. For cannula placement, the incised skin on the head was removed. Animals were then bilaterally implanted with guide cannulas that were custom made for individual target regions in the brain (P1 Technologies, USA). Dental acrylic, along with anchor screws fixed on the skull, was used for stably fixing the cannula implants. On termination of the surgical procedure, guide cannulas were covered with dummy cannulas, and maintained through the recovery period of 2-3 weeks. Dummy cannulas were removed only prior to drug administration on the day of the experiment. For acute delivery of drugs, an internal cannula attached to a Hamilton syringe (1 μL Microliter Syringe Model 7001 KH, Knurled Hub, 25-gauge, 2.75 in., point style 2) was used. The syringe was set on an infusion pump (PHD 22/2000 Syringe Pump, Harvard Apparatus, USA) that allowed controlled and precise delivery of the drug through the guide cannula. For viral infusion surgeries, virus vectors were injected in the target region using a Nanoject III Programmable Nanoliter Injector (Cat no: 3-000-207, Drummond Scientific Company, USA). All intracerebral viral infusions were performed at a constant flow rate of 100 nL/min (Total volume for rats: 800nL per hemisphere; total volume for mice: 500nL per hemisphere). After the infusion, the capillary was lifted up by 100 μm to release pressure and allowed to stay still for 8-10 minutes before removal. The incision on the scalp was closed using surgical sutures.

Headplate surgery

Animals injected with dexamethasone (3 mg/kg, i.m.; 002459, Henry Schein Animal Health, USA) were anesthetized with isoflurane (3%–4% for induction and 1%–2% for the remainder of surgery) and fixed in a stereotaxic apparatus (David Kopf Instruments), in contact with a water-circulating heating pad (Stryker Corp, USA) set to 37°C. Petrolatum ophthalmic ointment (Dechra Pharmaceuticals, UK) was used to cover the animal's eyes. The hair on the head was shaved, and the scalp was wiped and disinfected with ethanol and betadine. An incision was made to remove the skin, and the periosteum was cleared. A dental drill was used to make a 0.9 mm craniotomy and a 0.86 mm self-tapping bone screw (19010-10, Fine Science Tools, USA) was placed through the skull bone to act as a ground screw and provide further structural support for head-fixation. A stainless steel headplate was affixed on

the skull with C&B Metabond (Parkell, USA). All mice received carprofen (5 mg/kg, s.c. Zoetis, USA) as a postoperative analgesic immediately following surgery and for 3 days post-surgery. The targeted recording area was covered with silicon polymer. The mice were allowed to recover for at least one-week post-surgery prior to commencement of electrophysiological experiments.

Opto-tagging surgeries

Briefly, silicon probes were implanted as previously described.[73] Animals were anesthetized with isoflurane prior to craniotomy. A 64-channel silicon probe (NeuroNexus) was mounted on a micro-drive (Cambridge Neurotech) to allow accurate adjustment of the vertical position of the electrodes after implantation. A stainless-steel wire connected to a thin wire (California Wires) was inserted over the cerebellum and cemented in place with Metabond. A layer of Metabond was applied to the skull avoiding the craniotomy, thinner inside and thicker on the outer side of the skull forming a ring, over which four flaps of copper mesh were attached. The electrodes were then inserted right above the target region (aided by the micromanipulator), aimed at targeting CA1 (-2.9 mm posterior and 2.5 lateral from Bregma). Once in place, the microdrive was cemented over the skull, and probe had been inserted, the craniotomy was sealed with artificial dura-gel. Finally, the four flaps of copper mesh were bent upwards and soldered between them to provide stability and shielding the implant. The ground wire from the cerebellum was connected to the ground wires of the two electrodes and to the copper mesh.

Behavior assays

For the elevated plus maze (EPM) task, animals were placed in the center of the maze either facing the open arms or closed arms (chosen at random) and were allowed to freely explore the maze for ten minutes in the dark. The EPM for rats was built such that the two arms, both open and closed (45 cm x 10 cm each), were elevated 60 cm above the ground. The walls of the closed arms were 60 cm high. The elevated plus maze for mice was built such that the two arms, both open and closed (30 cm x 5 cm each), were elevated 50 cm above the ground. The walls of the closed arms were 15 cm high. The conjunction of the open and closed arms was deemed 'center area', which was defined by a 10 cm x 10 cm block for the rat maze, and 5 cm x 5 cm block for the mouse maze, and was excluded from analyses. A modified EPM was used to heighten the difference between the open and closed arms, by exposing the open arms to light intensity of more than 250 lux, whilst keeping the closed arms completely in the dark. Tracking was feasible only in the open arms since closed arms were occluded for video tracking. For analysis of anxiety-like behavior on open field test (OFT), the arena consisted of a box with dimensions (L x B x H) as follows: 100 cm x 100 cm x 60 cm for rats; 40 cm x 40 cm x 40 cm for mice. All animals were placed in the EPM or OFT 20 minutes after *i.p.* drug injection, or immediately after intracerebral drug infusion through the cannula. To assess whether the behavioral effects of DOI are persistent, animals were placed in the EPM 24 hours after treatment with DOI (Figures S1H–S1J). All behavioral assays for anxiety-like response were recorded for 10 minutes (expect Figures S1A–S1C, which was recorded for 15 minutes), tracked, and analyzed using the automated platform Ethovision XT 11 (Noldus).

Head twitch response (HTR) for experiments involving direct DOI infusion into the vHpc CA1/sub region were carried out with baselines determined 45 minutes prior to bilateral DOI delivery through the implanted cannula, and for a duration of 45 minutes upon DOI infusion. The number of HTRs were manually scored from recorded videos.

Electrophysiological recordings for neuropixels

Mice were habituated over several days to minimize restraint stress. At least two hours before recording, mice were anesthetized with isoflurane and 1mm craniotomy and durotomy as made over the target region to record from the ventral hippocampus. Cold (4°C) artificial cerebrospinal fluid (aCSF: 135 mM NaCl, 5 mM HEPES, 5 mM KCl, 1.8 mM CaCl2, 1 mM MgCl2; pH 7.3) was used to irrigate and clear the drilling debris as well as reduce heating of the underlying brain tissue. Care was taken to minimize bleeding and keep the area clear of bone fragments. A piece of Surgifoam soaked in aCSF and placed above the brain tissue was covered with silicon polymer to keep the craniotomy moist and clean prior to recording. A 22-gauge intravenous catheter system (B383323, BD Saf-T-Intima Closed IV Catheter Systems, Canada) was preloaded with DOI (1 mg/ml) and maintained at a neutral pressure. One hour prior to recording, mice were briefly anesthetized with isoflurane and implanted with the intravenous catheter to their intraperitoneal cavity and the catheter was fixed with a drop of Vetbond tissue adhesive (#1469, 3M Vetbond, USA). The mice were then head fixed and the catheter tubing was secured to the mouse holder tube with tape. Silicon polymer and Surgifoam were removed from the skull and craniotomies were briefly irrigated with aCSF. A Neuropixels 1.0 probe with the ground and reference shorted was coated in 10uL of CM-DiI (1mM in ethanol, Invitrogen, USA). The probe was then slowly lowered (~2um/s) into the brain to minimize tissue damage. The Neuropixels probe was inserted at the same stereotaxic coordinates as the behavioral experiments. The Neuropixels 1.0 probe is capable of recording from 960 sites over its 10-mm shank.[19] Due to wiring restraints, one can only record from 384 sites simultaneously. To maximize yield of units in ventral CA1, the default configuration for Neuropixels 1.0 recording was programmed to record from the 384 sites closest to the bottom of the probe. To determine units that are located in ventral CA1, the shank was coated with DiI and post-hoc visualization for the anatomical location of the probe trajectory was done using histology. For analysis, only the units that were located in ventral CA1 were used. Additionally, the local field potential recorded from the Neuropixels probe was examined to confirm directionality of pyramidal cell layer spike waveform, confirming that the sites are in the ventral CA1 layer and not in the dorsal CA1.

The probe was allowed to settle for at least 30 minutes before recording began. Data were acquired using the SpikeGLX software in external reference mode (https://billkarsh.github.io/SpikeGLX/). Action potential and local field potentials were recorded at 30 kHz

and 2.5 kHz, respectively. Once the recording began, 30 minutes of baseline activity was collected. The animal was then administered either 1 mg/kg of DOI or saline via the catheter and an additional 30 minutes of data were collected.

Electrophysiological recordings for opto-tagging

PV::ChR2 animals were implanted with a 64-channel silicon probe (Neuronexus or Cambridge Neurotech) with a custom glued multimodal optical fiber of 200 μm core (Thorlab FT200UMT) as previously described.[73] Pulses were generated with 50-ms, low intensity (0.5-2 mW) blue light[73] at 0.5 Hz. The pulse for stimulation was produced using an arbitrary waveform generator (Rigol, DG4062) to control a Laser Diode (Osram 470 nm wavelength) triggered by a current source (ThorLabs, LDC 240C). Intensity was manually adjusted during a few initial until optogenetic stimulation reliably produced a visible response in a subset of cells. An Intan RHD2000 interface board or Intan Recording Controller was used for recordings. The sampling rate used was set at 20000 Hz. Both amplification and digitization were done in the head stage (Intan Technologies). Data were visualized using the Intan recording software or Neuroscope (Neurosuite). LFP analyses were done in the down-sampled signal at 1250 Hz.

RNAscope experiments

Adult mice were anesthetized with isoflurane, and all brains were extracted and stored at -80°C prior to sectioning. Brains were sectioned at 16μm thickness using a cryostat (Leica CM 3050S) and collected on superfrost plus slides (Fisher Scientific, Cat. No. 12-550-15). Serial sections through the vHpc (Bregma coordinates: AP -3.00 and -4.00) were fixed on tissue slides using 4% PFA for 1 hour at room temperature. Sections were rinsed twice in 1% PBS followed by serial dehydration in ascending concentration of ethanol solutions. Experiments were performed using ACD kit (RNAscope® Multiplex Fluorescent Reagent Kit v2, Cat. No. 323100) as per manufacturer's instructions. Briefly, sections were pre-treated with H_2O_2 for 10 min at room temperature and then washed in distilled water. Sections were then dried and incubated with Protease IV prior to hybridization with specific probes: 5-HT_{2A} receptor (dilution:1:50; Mm-Htr2a-C2, Cat.No. 401291-C2), CamKIIα (dilution:1:50; Mm-Camk2a-C3, Cat. No. 445231-C3), and PV (dilution:1:1; Mm-Pvalb-C1, Cat. No. 421931-C1). Hybridization was carried out by incubating the tissue in a mix of the 3 probes for 2 h at 40°C followed by washes and exposure in 5% RNase-free SSC buffer (Invitrogen™, Cat. No. AM9770) overnight. Each probe was then individually and sequentially amplified at 40°C as follows: Mm-Pvalb-C1 and Mm-Htr2a-C2 for 30 min, and Mm-Camk2a-C3 for 15 min. Following washes, each probe was developed at 40°C using sequential steps of incubation in horseradish peroxidase (HRP) for 15 min, followed by incubation in fluorescent molecules (OPAL, Akoya Biosciences) for 30 min, with interim blocking steps (15 min) and washes during sequential probe development. Specific fluorescent molecules with defined wavelengths were associated with the individual target probes as follows: Mm-Pvalb-C1 (520 nm, green, Cat. No. FP1487001KT); Mm-Htr2a-C2 (570 nm, yellow, Cat. No. FP1488001KT); Mm-Camk2a-C3 (690, infrared, Cat. No. FP1497001KT). Sections were counterstained with DAPI to visualize cell nuclei (420 nm, blue) and mounted with coverslip using mounting medium (ThermoFisher Scientific, Prolonged Antifade Gold, Cat. No. P36930).

Immunohistochemical and histological analysis

Adult animals were injected with sodium thiopental prior to transcardial perfusion with PBS followed by 4% paraformaldehyde (PFA; Cat. No. 158127, Sigma-Aldrich). Brains were harvested and stored in 4% PFA for 48 hours. Coronal brain sections (50 μm) were generated on a vibratome (Leica Microsystems, Germany). Sections were permeabilized with PBS containing 0.3% Triton X-100 (0.3% PBSTx) for 1 hour and blocked with 0.3% PBSTx containing 10% horse serum (Cat. No. 26-050-088, Thermo Fisher Scientific, USA) for two hours at room temperature. The sections were then incubated with single antibodies or dual primary antibody cocktails as required: mouse anti-PV (1:500, Cat. No. P3088, Sigma-Aldrich), mouse anti-CamKIIα (1:200, Cat. No. 50049, Cell Signaling Technology), rabbit anti-c-Fos (1:1000, Cat. No. 2250S, Cell Signaling Technology), rabbit anti-5-HT_{2A}R (1:100, Cat. No. RA24288, Neuromics). Sections were subjected to serial washes with 0.3% PBSTx and were then incubated with secondary antibodies: donkey anti-mouse IgG conjugated to Alexa Fluor 555 or 488 (1:500; Cat. No. A-31570/A-21202, Invitrogen) or donkey anti-rabbit IgG conjugated to Alexa Fluor 555 or 488 (1:500; Cat. No. A-31572/A-21206, Invitrogen) for two hours at room temperature. After serial washes with 0.3% PBSTx, sections were mounted on slides using Vectashield Antifade Mounting Medium with DAPI (H-1200, Vector Laboratories) and images were visualized on a FV1200 confocal microscope (Olympus).

To localize the target areas following probe recording, mice were first deeply anesthetized with isoflurane prior to transcardial perfusion with PBS (Sigma-Aldrich) followed by 4% PFA (Sigma-Aldrich). The brain was extracted and fixed overnight in 4% PFA at 4°C. Subsequently, 50μm vibratome sections were collected, mounted on slides, and cover slipped with DPX. Images were taken at 10x magnification on an upright Leica DM5500 B microscope (Leica Microsystems). To align the DiI tracks left by the recording probe, we utilized SHARP-TRACK[74] to bridge our histology images onto the standardized Allen Common Coordinate Framework 6.[75] Reconstructed probe tracks were visualized within the Allen CCF using Brainrender.[76]

Western blotting

To assess 5-HT_{2A} receptor expression in the ventral hippocampus of the 5-HT_{2A}WT, 5-HT_{2A}KO, as well as PV-Cre::5-HT_{2A}RKO-res$^{fl/fl}$ bigenic mice, we conducted western blotting analysis. Ventral hippocampal tissues were dissected and mechanically homogenized in radioimmunoprecipitation assay buffer (50 nm Tris-Cl, pH 8.0, 5 mm EDTA, 1% NP-40, 150 mm NaCl). Protein concentration was

estimated with the QuantiPro BCA Assay Kit (Sigma-Aldrich), and lysates were resolved on a 10% SDS polyacrylamide gel before transfer onto polyvinylidene fluoride membranes. Blots were subjected to blocking in 5% milk/BSA in TBST and incubated overnight with the following primary antibodies: rabbit anti-5-HT_{2A} (1:1500) and rabbit anti-β-actin (1:12,000). Blots were exposed to HRP-conjugated goat anti-rabbit secondary antibody (1:8000) in 1% milk/BSA for 1 h. Signal was visualized on an Imager 800 (GE Healthcare) using a western blotting detection kit (WesternBright ECL, Advansta).

QUANTIFICATION AND STATISTICAL ANALYSIS

Statistics for behavioral, immunofluorescence, and RNAscope assays

All experiments that had two treatment groups were subjected to a two-tailed, unpaired Student's t test using GraphPad Prism (Graphpad Software Inc, USA), following confirmation of normal distribution of data using the Kolmogorov-Smirnov test on GraphPad Prism. Welch's correction was applied when a significant difference in the variance between groups that were normally distributed was observed. F-values for Student's t test with $p<0.05$ have been indicated in the figure legends. For data that did not follow a normal distribution, the Mann-Whitney-U-test was applied for group comparison, and where applicable the p value for Kolmogorov-Smirnov test is indicated in the figure legends. Experiments with four groups and two variables were analyzed with a two-way analysis of variance (ANOVA), followed by the application of Bonferroni's *post-hoc* test when a significant two-way interaction was determined. Data with four groups and one variable was analyzed with a one-way ANOVA, followed by the application of Tukey's *post-hoc* test when a significant interaction was determined. Paired t test was used to analyze HTR results with comparisons made between baseline HTR and DOI-evoked HTR per animal. All data are expressed as mean ± standard error of the mean (S.E.M) and statistical significance was set at $p \leq 0.05$.

Electrophysiological analysis for neuropixels recordings

A custom python script (https://github.com/jenniferColonell/ecephys_spike_sorting), was used to preprocess raw data, spike sort data (via Kilosort), calculate mean waveform and quality control metrics. Putative single units identified by Kilosort 2.0 were manually curated in Phy (https://github.com/kwikteam/phy). To identify parvalbumin interneurons, we utilized the spike width duration (ms) to separate our recorded neurons into putative fast-spiking interneurons and regular spiking neurons. Spike width duration has been used extensively across brain areas to separate fast-spiking and regular-spiking neurons. Spike width was defined as the duration of time between the trough and the peak, with a selected threshold of 0.4 ms based on prior studies in the hippocampus that has classified units using spike widths and other waveform features.[77] To determine changes in firing rate activity, the z-score for each neuron was calculated relative to its baseline activity during the pre-drug infusion period (0–30 minutes). To determine whether a neuron's activity was significantly modulated by either saline or DOI we calculated the fraction of neurons that had significantly modulated z-scores ($\geq$5 for increased, $\leq$ 5 for decreased) over the length of the recording. Binomial tests were conducted at each time point to determine if a notable portion of neurons increased or decreased their firing rate, statistical significance was set at $p \leq 0.01$.

Spike sorting and single-unit classification for opto-tagging experiments

Spike sorting was performed semi-automatically using KiloSort[78] (https://github.com/cortex-lab/ KiloSort), followed by manual curation using the software Phy (github.com/kwikteam/phy) and custom designed plugins to obtain well-isolated single units (https://github.com/petersenpeter/phy-plugins). Cluster quality was assessed by manual inspection of waveforms and auto-correlograms, and by the isolation distance metric. Multiunit, noise clusters, or poorly isolated units were discarded from the analysis. Well-isolated units were classified into putative cell types using the Matlab package Cell Explorer (petersenpeter.github.io/Cell-Explorer).[79] Spiking features such as auto-correlogram, spike waveform, and putative monosynaptic connections derived from short-term cross correlograms, were used to select, and characterize well-isolated units. All well-isolated units were classified into three cell types as shown in previous work[80,81]: putative pyramidal cells, narrow waveform interneurons, and wide waveform interneurons. The two key metrics used for this separation were burst index and trough-to-peak latency.[82] Burst index was determined by calculating the average number of spikes in the 3–5 ms bins of the spike autocorrelogram divided by the average number of spikes in the 200–300 ms bins. To calculate the trough-to-peak latency, the average waveforms were taken from the recording site with the maximum amplitude for the averaged waveforms of a given unit. For further quantifications, well-isolated cells with at least 100 spikes in a given session were included in the analyses.

Cells were identified as PV-positive interneurons if they reliably increased their firing rate, with low latency (< 3 ms from pulse onset) and minimal jitter, in response to light pulses. Firing rate increase was computed within light pulses compared to randomly selected 50 ms windows outside pulse timings (Wilcoxon rank test, $p<0.05$). Responsive cells were additionally identified as narrow waveform interneurons based on auto-correlogram, spike waveform, and firing rate characteristics. Putatively opto-tagged units were also visually verified to ensure they showed a clear increase in firing aligned with pulse onset, terminating only at the offset of the pulse. A minority of other neurons displayed heterogeneous responses to stimulation (either decrease or increase in firing rate) but with much higher latencies and jitter and lower trial-by-trial reliability, that could reflect polysynaptic activation. These neurons were not labelled as identified PV-positive cells.

Please cite this article in press as: Tiwari et al., Ventral hippocampal parvalbumin interneurons gate the acute anxiolytic action of the serotonergic psychedelic DOI, Neuron (2024), https://doi.org/10.1016/j.neuron.2024.08.016

Brain state detection

Brain state scoring was performed as previously described.[71] The local field potential (LFP) was extracted from the wide-band data using a lowpass filter (sync filter with a 450 Hz cutoff) and down-sampling to 1250 Hz. The broadband LFP, narrow-band theta frequency LFP, and estimated electromyogram (EMG) were used in combination for state scoring. Spectrograms were generated from the LFP with a fast Fourier transform using 10 second sliding windows (at 1 second). A z-transform was performed, followed by principal components analysis. The first principal component extracted reflected power in the lower (<20 Hz) frequency range, whereas later components reflected higher (>32 Hz) frequencies. Theta dominance was quantified by taking the ratio of power between 5-10 Hz and 2-16 Hz frequency bands. EMG was estimated as the zero-lag correlation between the 300-600 Hz filtered signals across recording sites.[83] States with a high LFP principal component 1 and low EMG were considered non-REM; high theta periods with low EMG were considered REM; the remaining periods were classified as the waking state.

Sharp wave ripple detection and spike content analysis

For sharp wave ripple (SWR) detection, the wide-band signal from a CA1 pyramidal layer channel was filtered (difference-of-Gaussians; zero-lag, linear phase FIR), and instantaneous power was calculated by clipping at four standard deviations (SDs), rectified, and lowpass filtered.[73,80,81] The low-pass filter cut-off was at a frequency corresponding to p-cycles of the mean bandpass (for 80-250 Hz band-pass, the low-pass was 55 Hz). Subsequently, the power of the non-clipped signal was computed, and all events exceeding fours SDs from the mean were detected. The events were then expanded until the non-clipped power fell below one SD; short events (<15 ms) were discarded. Sharp waves were detected separately using LFP from a CA1 str. radiatum channel, filtered with band-pass filter boundaries (5-40 Hz). LFP events of a minimum duration of 20 ms and a maximum of 400 ms exceeding 2.5 SD of the background signal were included as candidate SWRs.

Electrophysiological analysis for opto-tagging recordings

To determine changes in firing rate activity induced by DOI injection, each neuron response was calculated relative to its baseline activity during the pre-drug infusion period (0–30 minutes). To control for differences in firing patterns across different brain states, each neuron firing rate was binned into 15 second bins and z-score based on firing within the same brain state during the pre-drug infusion period. We considered that a neuron's firing rate was significantly modulated by either saline or DOI injections if it displayed a change above or below 5 z-scored units in the 30 minutes post injection compared to baseline. We then pooled all significantly modulated units for each cell type and condition. Binomial tests were conducted at each time bin to determine if a significant fraction of neurons increased or decreased their firing rate post-drug, statistical significance was set at $p \leq 0.01$.